THE EFFECT OF NUTRIENT LIMITATION AND OXIDATIVE STRESS ON BROMOFORM PRODUCTION FROM AXENIC CULTURES OF MARINE DIATOMS

By

Mariam Nguvava

A thesis submitted as part of the requirement for the degree of Master of Science in Applied Marine science. In the Oceanography Department, Faculty of Science, University of Cape Town.

July, 2012

DECLARATION

I, Mariam Nguvava, I declare that this thesis is my own work. It has not submitted for any examination in any other University. All the source (s) contributed to make this work has been cited and referenced.

Signature:

Date

ACKNOWLEDGEMENTS

The success of this study would not be possible without a scholarship from the German Academic Exchange Service (DAAD). Thanks for giving me this opportunity. Thanks also to ICEMASA (International Centre for Education, Marine and Atmospheric Sciences over Africa) for funding the experiments.

My sincere thanks to my supervisor Dr. Eva Bucciarelli for helping me at each step of this thesis (God bless you always). I am also grateful to my supervisors, Dr. Howard Waldron, and Dr. Carl Palmer.

Miss Raïssa Philibert and Mr. Brett Kuyper (PHD students-Oceanography), thanks for your help. Special thanks also to the people at the marine aquarium (South Africa) for their help and the facilities they provided during experiment.

Special thanks to my beloved friend and workmate, Saiguran Loisulie (Rest in Peace). I will always remember you.

To my beloved mother (Zuhura), step father (Mohammed) and sisters (Zainab and Zulpha). Thanks for your prayers and encouragements!

ABSTRACT

Bromoform is a source and an important carrier of non-volatile reactive bromine in the troposphere and stratosphere. In the atmosphere free bromine atoms catalytically react with ozone. This causes decrease in ozone concentration which is an important green-house gas and UV shield. Bromoform is mainly produced naturally by marine organisms. The production by microalgae however is not well quantified, and the mechanism by which phytoplankton produce bromoform is not fully elucidated. The production of this compound at the cellular level seems to be linked to oxidative stress via the use of the antioxidant enzyme bromoperoxidase (Manley and Barbero, 2001). However, no experiment has been conducted under bacteria-free conditions, which may bias the results because bacteria produce bromoform. Diatoms, which are wide spread in the open ocean, could be amongst the most important producers of bromoform.

The purpose of this study was to quantify the effect of nutrient limitation and oxidative stress on bromoform production from axenic cultures of marine diatoms. Semi continuous cultures of *Phaeodactylum tricornutum* (*P. tricornutum*) and *Chaetoceros neogracile* (*C. neogracile*) were grown in f/2 medium under continuous light conditions. The experiment was divided into three subsections: 1) Exponential phase, where the cultures were fully enriched with nutrients 2) Carbon dioxide (CO_2) limitation, where CO_2 deficiency was induced by addition of sodium hydroxide (NaOH) and 3) Nitrate (NO_3^-) limitation, where the cultures were grown without NO_3^-.

The result show high bromoform production when the cultures were in exponential phase. Average production was 9.0×10^{-18} mol cell^{-1} for *P. tricornutum* and 16.5×10^{-18} mol cell^{-1} for *C. neogracile*. Production rate was 11.4×10^{-18} mol cell^{-1} day^{-1} for *P. tricornutum* and 28.0×10^{-18} mol cell^{-1} day^{-1} for *C. neogracile*. Bromoform per cell and per cell per day decreased during CO_2 limitation by ~2 times and 4 times for *P. tricornutum* respectively, and ~5 times and 20 times for *C. neogracile* respectively. No bromoform was produced by the nitrate limited cells of *P. tricornutum*.

Based on these results, it can be hypothesized that the decrease of bromoform production during CO_2 limitation and its absence during nitrate limitation might be due to the decreased concentration or activity of the antioxidant enzyme bromoperoxidase that produces bromoform. Because the enzyme is made up of protein (nitrogen), any condition limiting nitrogen uptake (CO_2 limitation or nitrate limitation) may decrease its concentration or activity.

TABLE OF CONTENTS

LIST OF FIGURES

LIST OF TABLES

CHAPTER 1

INTRODUCTION

1.1 Atmosphere layers

The atmosphere is composed of four distinct layers; the troposphere, the stratosphere, the mesosphere, and the thermosphere (Figure 1.1). The layers differ, among major properties, in terms of distance from the Earth surface (measured at sea level), gaseous composition and concentration, temperature and pressure.

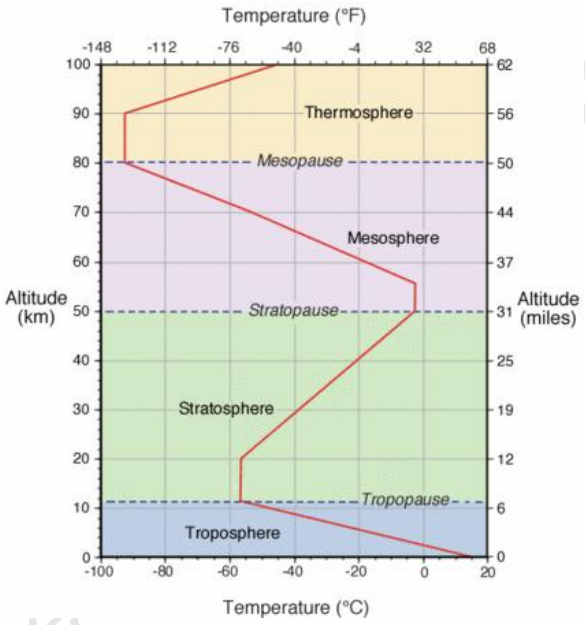

Figure 1.1: Atmospheric layers

(http://www.eoearth.org/article/Atmosphere_layers)

One of the interesting feature shared between troposphere and stratosphere is the presence of ozone (O_3) (Krupa and Manning, 1988). It is a naturally occurring gas. The stratosphere is known to account for almost 90% of the vertical O_3 column above the earth's surface. The troposphere accounts for an additional 10% (Krupa and Manning, 1988) (Figure 1.2).

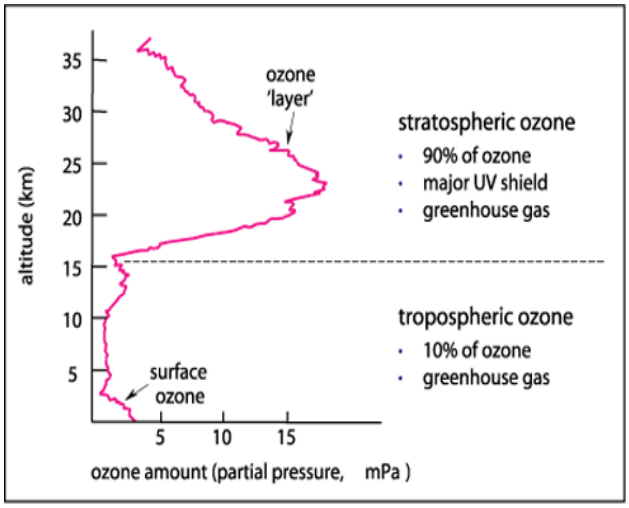

Figure 1.2: Vertical distribution of ozone in the atmosphere at mid-latitudes (http://www.environment.gov.au/soe/2001/publications/theme-reports/atmosphere/pubs/part04.pdf).

1.2 Ozone natural cycle

Ozone is a minor component (0.02 – 0.1 part per million based on volume (ppm_v)) of the Earth's atmosphere (Pidwirny, 2006), however it has a significant role in filtering the Sun's ultraviolet (UV-B) radiation (Krupa and Manning, 1988; Wang et al., 1995). This role is mainly achieved by ozone found in the stratosphere (Figure 1.2). Unfiltered UV radiation, being of short wavelength and hence highly energetic, can destroy animal and plant tissues. Also, ozone is a greenhouse gas (similar to H_2O, CO_2, CH_4, CFC's and N_2O) which traps outgoing long wave radiation from the Earth's surface. This process maintains the Earth temperature at ~ 15°C (Wang et al., 1995; Lacis et al., 1990).

In a natural cycle, ozone is constantly destroyed and produced. This process creates equilibrium ozone concentration. The elementary reactions (of ozone production and destruction) which constitute the Chapman cycle (Chapman, 1930) are;

$$O_2 + h\nu \longrightarrow 2O \qquad (1.2\text{-}1)$$

$$O + O_2 + M \longrightarrow O_3 + M \qquad (1.2\text{-}2)$$

$$O_3 + h\nu \longrightarrow O + O_2 \qquad (1.2\text{-}3)$$

$$O + O_3 \longrightarrow 2\,O_2 \qquad (1.2\text{-}4)$$

M is any non-reactive species. It is either oxygen (O_2) or nitrogen (N_2) as these are the major components of the atmosphere. M takes up the excess energy released in reaction (1.2-2) to stabilize O_3 formed. Hence, M slows down reaction (1.2-3). The destruction of O_3 occurs by excitation UV radiation, which releases oxygen atom (O) and oxygen molecule (O_2) (1.2-3). The reaction between O and O_3 produce O_2 and complete the cycle of ozone formation and destruction (Figure 1.3).

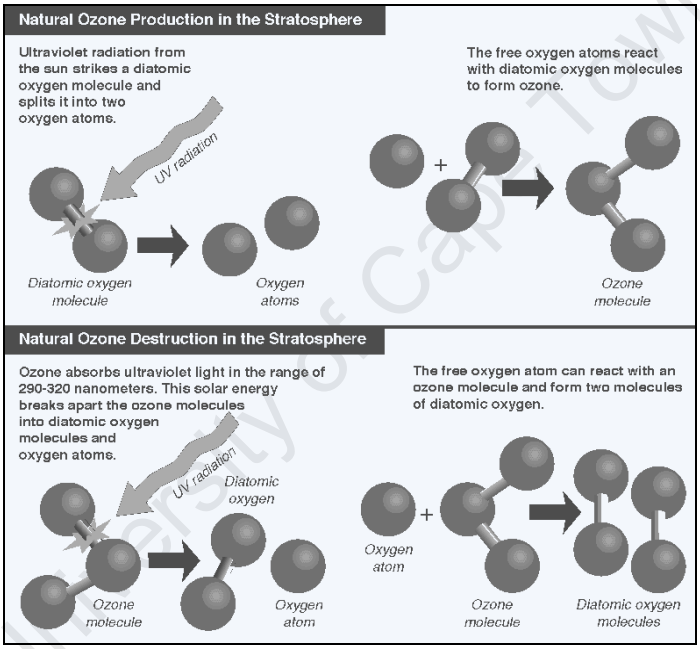

Figure 1.3: Ozone natural cycle
(http://www.ozonedepletion.info/education/ozone.html)

Tropospheric ozone, or "ground ozone", results from two major sources: a) Low concentrations are transported from the lower level of the stratosphere to the troposphere and b) Photochemical oxidation of hydrocarbons and carbonmonoxide (CO) in the presence of nitrous oxides radicals (NO_x : $NO+NO_2$) directly produces O_3 in the troposphere (Guicherit and Roemer, 2000: Liu et al.,

2002). Natural sources of hydrocarbons, CO, and NO_x are the vegetation, microbial activity in soils, and lightning (Liu et al., 2002).

1.3 Reactions of bromine with atmospheric ozone

Both stratospheric (Wang et al., 1980; Yung et al., 1980; Anbar et al., 1996; Sturges et al., 2000) and tropospheric (Oltmans et al., 1989; Bottenheim et al., 1990; Dvortsov et al., 1999; Sturges et al., 2000; Yang et al., 2005) ozone is destroyed. The destruction can be due to the reactions of ozone with halogens (*e.g.* chlorine and bromine) (equations 1.3-1 and 1.3-2) (Wang et al., 1980).

$$Br + O_3 \longrightarrow BrO + O_2 \qquad (1.3\text{-}1)$$

$$Cl + O_3 \longrightarrow ClO + O_2 \qquad (1.3\text{-}2)$$

The presence of bromine in the troposphere and lower stratosphere upsets the natural equilibrium of ozone by destroying it faster than it is naturally produced. As a result, ozone concentration decreases (Anbar et al., 1996; Dvortsov et al., 1999; Sturges et al., 2000; Yang et al., 2005). Bromoform is among the species containing bromine that can affect O_3 concentration.

Bromoform ($CHBr_3$) is a chemical compound made up of one carbon atom covalently bonded by one hydrogen and three bromine atoms (Figure 1.4).

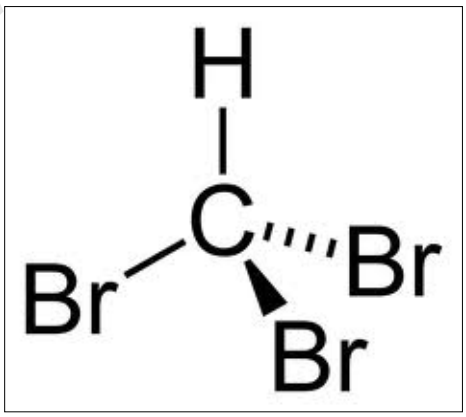

Figure 1.4: Chemical structure of bromoform
(http://chemistry.about.com/od/chemistryglossary/g/Organobromide)

It is a source and an important carrier of non-volatile reactive bromine into the troposphere and lower stratosphere (TLS) (Bottenheim et al., 1990; Dvortsov et al., 1999; Fahey and Ravishankara, 1999; Sturges et al., 2000). Bromine can indeed be produced by the photolysis of bromoform. Bromoform undergoes photolysis in two steps as shown by MCGivern et al. (2002) in equations 1.3-3 and 1.3-4.

$$CHBr_3 \xrightarrow{h\nu} CHBr_2\bullet + Br\bullet \qquad (1.3\text{-}3)$$

$$CHBr_2\bullet \xrightarrow{h\nu} CHBr\bullet + Br\bullet \qquad (1.3\text{-}4)$$

This results to production of free bromine radicals which then react with hydroxyl radicals to produce reactive bromine species (BrO_x: Br+BrO) (Figure 1.5).

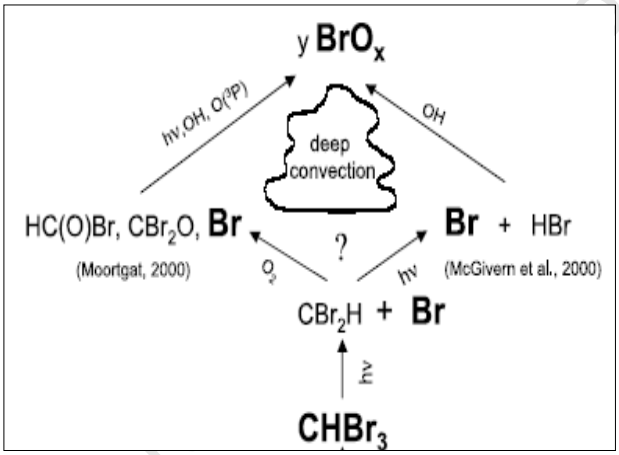

Figure 1.5: Photolysis and oxidation of bromoform in the atmosphere (Quack and Wallace, 2003)

In the atmosphere, bromoform photolysis and reaction with OH radicals estimated to have a life time of 35 to 100 days (Quack and Wallace, 2003). Bromine oxide (BrO) catalytically destroys ozone (equations 1.3-5) or can react with Chlorine oxide (ClO) to form extra reactive halogens (Br and Cl) (equations 1.3-6) (Yung et al., 1980).

$$BrO + O_3 \longrightarrow Br + 2O_2 \qquad (1.3\text{-}5)$$

$$BrO + ClO \longrightarrow Br + Cl + O_2 \qquad (1.3\text{-}6)$$

Bromoform is considered the second most reactive organobromine gas, after methyl bromide, in the background troposphere (Sturges et al., 2000). This is because of its three bromine atoms which are creating the potential for reactive bromine. Compared to other brominated volatile compounds like methyl bromide, bromoform has a short life-time (< 0.3 years) (Quack and Wallace, 2003) in the atmosphere. It contributes more to the addition of bromine atoms into the lower troposphere (LT) than into the upper troposphere (UT) and lower stratosphere (LS) (Dvortsov et al., 1999; Sturges et al., 2000). Methyl bromide has a longer atmospheric life-time (between 0.8 to 2 years) (Honaganahalli and Seiber, 1997) and is able to carry bromine atoms into the stratosphere (Wofsy et al., 1975). However, supersaturation, high fluxes, high marine boundary layer mixing ratios, and intense convection processes in the troposphere, can transport bromoform into the UT and LS as well (Yang et al., 2005; Salawitch, 2006; Butler et al., 2007).

Other organohalogen compounds like organochlorines, organofluorines and organoiodines can also produce halogen radicals by photolysis and contribute to the total destruction of ozone. Organochlorine is the most abundant in the atmosphere (especially stratosphere) (Wuosmaa and Hager, 1990) and hence can have a higher impact on stratospheric ozone concentrations. However, the concentration of bromoform is higher in the troposphere, and dominates ozone destruction in this layer. It should be noted that, bromine radicals are ~50-60 times more efficient than chlorine radicals in depleting atmospheric ozone (World Meteorological Organization (WMO), 1999). Because of its effectiveness, the low concentration of bromoform in the stratosphere results in a significant reduction of ozone.

Studies on atmospheric concentration of bromine from bromoform have been conducted using both models and measurements (Dvortsov et al., 1999; Sturges et al., 2000). Pronounced increases in the concentration of bromine radicals in the TLS have been observed in recent years (Dvortsov et al., 1999; Bridgeman et al., 2000; Nielsen and Douglass, 2001) and are attributed to an increase in bromoform concentration in the troposphere (Dvortsov et al., 1999; Nielsen and Douglass, 2001). This bromoform is rapidly transported, through convective transport, to

the lower stratosphere (LS) (Quack and Wallace, 2003; Salawitch, 2006). Dvortsov et al. (1999) used a two-dimensional (2-D) model with convective transport derived from the three-dimensional (3-D) NCAR Community Climate Model version3 (CCM3) to model the stratospheric bromine concentration attributed to the photolysis of bromoform. This study showed that about 1 ppt Br at 12 km altitude at mid-latitudes originated from bromoform and only 0.5 ppt Br was from long-lived sources (like methyl bromide). Sturges et al. (2000) measured bromoform concentrations of 0.1 to 1 ppt in the upper troposphere and ~0.01 ppt in the lower stratosphere. Both natural and anthropogenic sources of bromoform are detailed below.

1.4 Sources of bromoform

1.4.1 Anthropogenic sources of bromoform

The anthropogenic sources represent a minor contribution of bromoform (~0.3 x 10^{10} $gCHBr_3yr^{-1}$) in the atmosphere, compared to the annual global flux (~10 x 10^{11} $gCHBr_3yr^{-1}$) (Quack and Wallace, 2003). However, locally, anthropogenic production of bromoform may need to be taken into consideration (Quack and Wallace, 2003). The anthropogenic sources of bromoform emission in the atmosphere are through disinfection processes of seawater, freshwater and wastewater (Warwick et al., 2006). The main anthropogenic sources are considered to be located in dense urban and agriculture regions (Goodwin et al., 1997a).

1.4.2 Natural sources of Bromoform

Bromoform is one of the structurally simplest of the naturally produced organobromine compounds (Paul and Pohnert, 2011). Recent researchers focused on natural sources of bromoform production because of their high contribution to atmospheric bromine concentrations and ozone depletion. Marine sources represent about 90% of the global bromoform production (Warwick et al., 2006). It is estimated that about 2-6 x 10^{11} g $CHBr_3yr^{-1}$ of global biogenic flux of bromoform is from the ocean (Fogelqvist and Krysell, 1991), with variability between the tropics and high latitudes. Ozone destruction is predominantly observed at the higher latitudes (polar regions) (Paul and Pohnert, 2011; Xu et al., 2002) which resulted in a focus on bromoform emissions in the Arctic and

Antarctic regions (Manley et al., 1992; Moore et al., 1996; Laturnus et al., 1996; Scarratt and Moore, 1996). However, recent studies by Quack and Wallace (2003); Butler et al. (2007); Colomb et al. (2008); Hence and Quack (2009); revealed the tropical ocean as a potential source of bromoform to the atmosphere, therefore there is much potential for research in this region.

Bromoform has a low solubility and is readily out-gassed into the marine atmosphere boundary layer (MABL) (Carpenter and Liss, 2000). The MABL is that part of the atmosphere which is directly in contact with the ocean. In this layer, ocean and atmosphere exchanges large quantities of heat, moisture, and momentum mainly through turbulent transport. Observation of bromoform both in the air and sea water in the tropical and temperate regions of the Pacific and Atlantic Ocean has been documented in different studies (*e.g.* Atlas et al., 1993; Schauffler et al., 1999; Quack and Wallace, 2003; Butler et al., 2007). Yokouchi et al. (2005) measured the concentration of bromoform in the tropical region of Pacific Island coasts and described this region as an important bromoform source. Modeling studies by Palmer and Reason, (2009) also obtained peaks of bromoform in the air above Pacific Ocean. Carpenter and Liss (2000) estimated a bromoform global flux of ~2.2 x 10^{11} g yr^{-1} by combining fluxes from temperate macroalgae and microalgae. To improve the estimate of fluxes from the ocean to the atmosphere, the oceanic sources of bromoform must be investigated repeatedly.

1.5 Bromoform production by marine organisms

Marine organisms (like algae and bacteria) naturally produce bromoform (Gribble, 1999). Compared to other marine organisms, algae have been described as the most dominant group producing large quantity of bromoform (Paul and Pohnert, 2011). Both macroalgae (seaweeds) and microalgae (phytoplankton) add significant amounts of bromoform to the marine environment (Manley, 2002). Globally, macroalgal production of bromoform is estimated to be (0.3-2.3) x 10^{11} g yr^{-1}, while that of microalgae is estimated at (0.1-1.5) x 10^{11} g yr^{-1} (Carpenter and Liss, 2000). Although seaweeds are generally considered as the dominant source of bromoform, the uncertainties that exist in the values given mean that microalgae may be an important source of this compound (Manley et al., 1992;

Goodwin et al., 1997a; Carpenter and Liss, 2000). Bromoform concentrations at the surface ocean or in the atmosphere vary temporally and spatially. The sources of production, together with the pathways through which they were synthesized, are among the factors which can contribute to spatial and temporal variability (Quack and Wallace, 2003).

1.5.1 Macroalgae (Seaweeds) sources:

Different species of macroalgae (brown, green and red algae) produce different concentrations of bromoform (Gribble, 2003; Paul and Pohnert, 2011). In a study conducted along the Arctic Ocean by Laturnus (1996), it was observed that brown and green algae have higher rate of bromoform production compared to red algae. Bromoform production by tropical and subtropical seaweed species is higher than production by high latitude seaweed species (Scarratt and Moore, 1998; Quack and Wallace, 2003). The near shore waters of the subtropical regions have highest concentrations of bromoform (~>300 ppt), followed by the Arctic waters (~90 ppt) and the Antarctic Ocean (~18 ppt) (Quack and Wallace, 2003). Also the Pacific and Atlantic Ocean species produce bromoform at different rates. Laboratory observations showed that the rate of production was higher (5-40 times) for the Pacific Ocean macroalgae species (Manley et al., 1992) than the Atlantic species (Gschwend et al., 1985). Manley et al. (1992) conducted both laboratory and field measurements along the coasts of southern California on macroalgae bromoform production. It was found that the rate of bromoform production was higher for kelp species than non-kelp species.

Global production of bromoform by seaweeds is restricted to the coastlines (Goodwin et al., 1997a; Manley et al., 1992). Therefore, not surprisingly, the highest marine concentrations of bromoform are found in coastal waters (Manley et al., 1992; Goodwin et al., 1997a; Carpenter and Liss, 2000; Welter et al., 2002) with decreasing concentrations towards the open ocean (Figure 1.6).

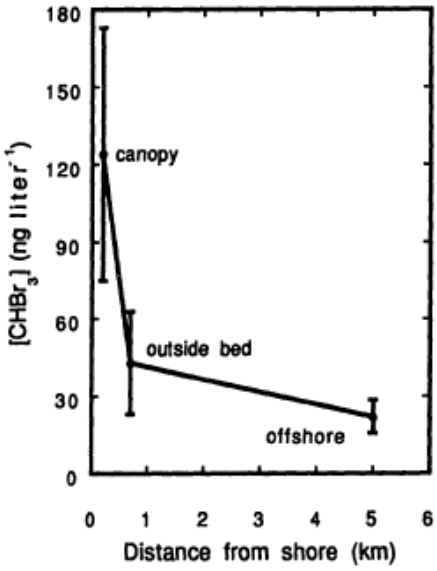

Figure 1.6: Bromoform ($CHBr_3$), surface seawater concentrations (± SD) as a function of distance from shore**.** Samples were collected from the coastal sites of Orange Country, California on 14 August 1990 (Manley et al., 1992).

According to Quack and Wallace (2003), bromoform concentration can be up to 100 times higher in the coastal and shelf regions than in the open ocean. However, because of seaweeds' locality, their impact on bromoform production has more effects at the local than the global level (Goodwin et al., 1997a).

Bromoform production by macroalgae is also affected by seasonal variability. The variability may occur due to nutrient depletion in waters above the thermocline, algal physiological state (visible degradation), and light conditions. For example Goodwin et al. (1997a) observed the highest production of bromoform by brown macro algae during mid-summer (July-August) (Figure 1.7). This was related to the poor physiological state of the seaweeds.

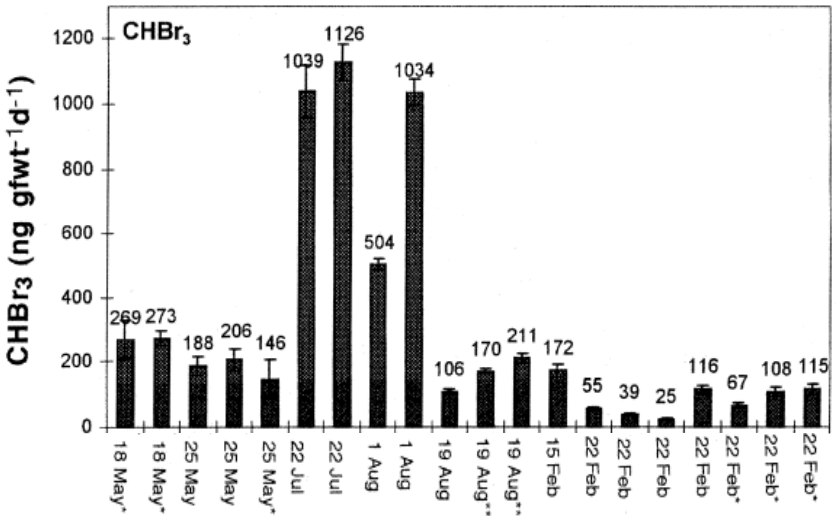

Figure 1.7: Production rates of bromoform for macroalgae (*M. pyrifera*) at different seasons (Goodwin et al., 1997a). Error bars are ± 1 SE of regression. Samples collected between May 1994 to February 1995 at Laguna Beach and Dana point, California.

Bromoform production by macro algae species in the subtropical and temperate regions also varies with light. Based on the study conducted by Goodwin et al. (1997a) and Carpenter and Liss (2000), maximum production of bromoform was found to occur during day time (Figure 1.8).

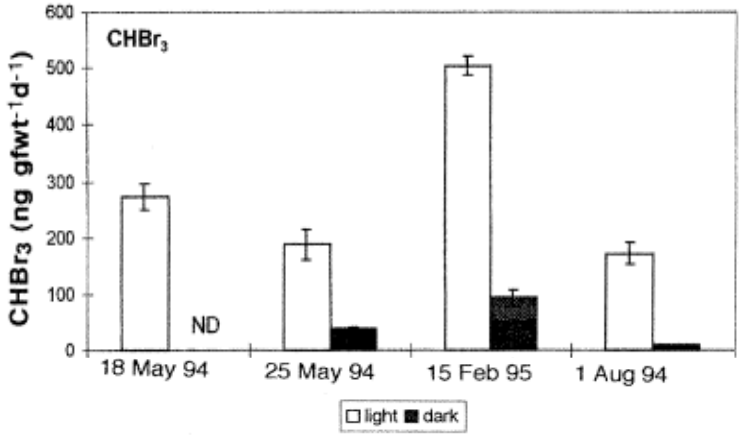

Figure 1.8: Production rates of bromoform for macroalgae (*M. pyrifera*) under light and dark conditions (Goodwin et al., 1997a). ND= no detection of bromoform production. Error bars are ± 1 SE of regression.

1.5.2 Microalgae (Phytoplankton) sources

While kelp is coastally constrained, as it needs rocks in order to root upon, phytoplankton are found throughout the world's oceans (both coastally and open ocean). Since they cover a much larger area they may be able to contribute significantly to the atmospheric bromoform budget (Scarratt and Moore, 1996) (Figure 1.9).

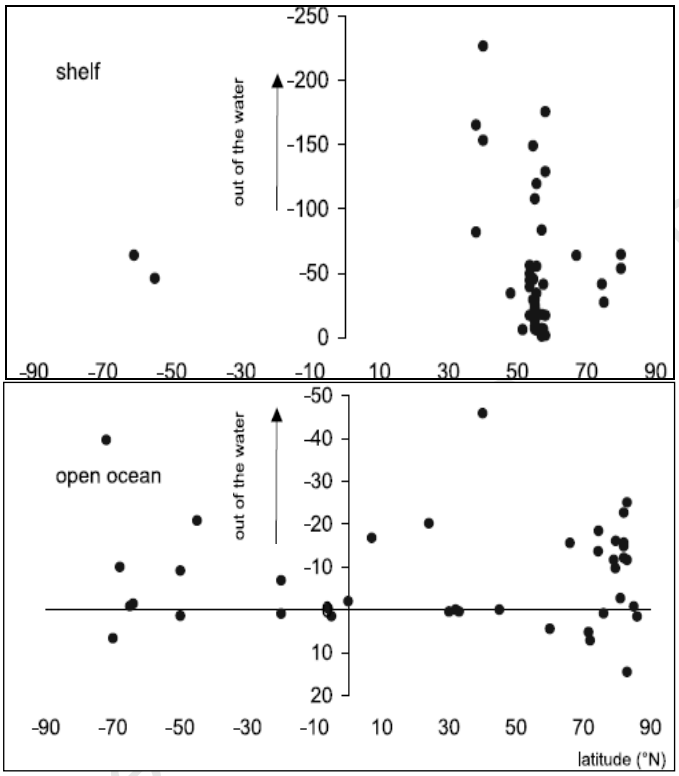

Figure 1.9: Change in bromoform concentration (pmol L^{-1}) between sea surface and air (as a function of latitude) for the shelf and open waters by Quack and Wallace (2003). The shelf source is mainly due to the macroalgae while the open ocean source is mainly due to the phytoplankton.

Butler et al. (2007) concluded that phytoplankton in the open ocean was the main source of bromoform in this area. Production of bromoform by different species of phytoplankton varies widely, *e.g.* ice diatoms produce more bromoform (Moore et al., 1993; Tokarczyk and Moore 1994; Moore et al., 1996) than temperate diatoms (Moore et al., 1996; Colomb et al., 2008).

Correlation of phytoplankton biomass (as a function of chlorophyll *a*) and bromoform production is also of great importance. Chuck et al. (2005) showed that there was a weak correlation between bromoform and chlorophyll *a* concentrations in the open ocean. A possible reason for this observation is that bromoform production is species dependent (Moore et al., 1996) and using the biomass of different species cannot provide a good estimate of bromoform production.

Another important observation is the tendency of bromoform concentration to decrease with depth (Krysell, 1991; Butler et al., 2007) (Figure 1.10).

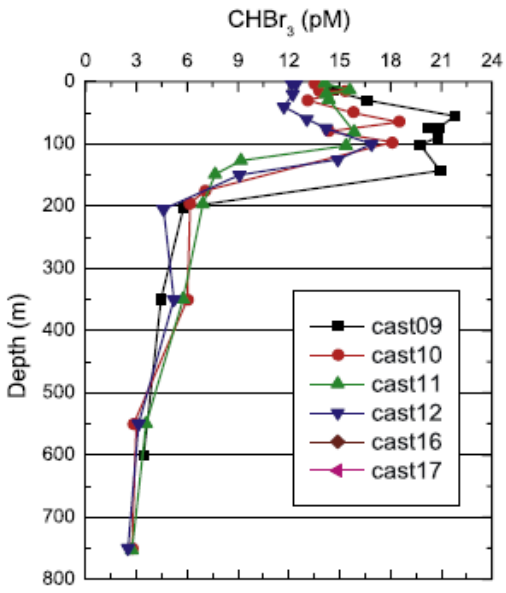

Figure 1.10: Variation of bromoform with depth in the open ocean from Butler et al. (2007). Data collected from seven cruises over 10 year span in the Pacific, Atlantic and Southern Ocean.

This phenomenon is controlled by phytoplankton activity which is concentrated in the euphotic layer of the ocean (Manley et al., 1992; Goodwin et al., 1997a). However, in some cases, it is possible to find increasing concentration of bromoform with depth in the open ocean. This could be due to the transport of coastal waters rich in bromoform to the open ocean (Carpenter and Liss, 2000).

The reasons why many of these organisms produce organobromine compounds are still not fully understood. However, in most of the marine algae, production of bromoform is considered to serve as a chemical defence against micro-organisms (MCConnell and Fenical, 1977) and herbivores (Gschwend et al., 1985), or as a by-product of an antioxidant system due to excess production of reactive oxygen species, specifically hydrogen peroxide (H_2O_2) in their cells (Collén et al., 1994). There are different cellular pathways for the production of bromoform.

1.6 Metabolic processes of bromoform production

Moore et al. (1996) showed that the formation of bromoform and bromine containing compounds in phytoplankton is due to the activity of the enzyme bromoperoxidase. Acting as an anti-oxidant system, bromoperoxidase may catalyze the reactions of antioxidants (i.e. Iodine, bromine), which have the potential of damaging oxidant H_2O_2. Potential sources of H_2O_2 are through biological metabolic pathways which include reactions of photosynthesis, mitochondrial respiration, and enzymatic catalysis of certain H_2O_2 yielding reactions (Manley, 2002). Accumulation of H_2O_2 results in cell damage (Manley and Barbero, 2001; Lesser, 2006), including the destruction of lipids, protein and deoxyribonucleic acid (DNA). Antioxidants like bromoperoxidase react with H_2O_2 and detoxify the cell from this harmful compound. Wever et al. (1991); Moore et al. (1996); Goodwin et al. (1997a); Manley (2002) suggested that, bromoperoxidase produces bromoform as a result of catalyzing halide oxidation in the presence of surplus H_2O_2 in the cells. After being produced bromoform diffuses out of the cells.

Bromoform metabolism can be achieved through different pathways. The major pathway involves the oxidation of bromide to hypobromite. Bromide oxidation is the major source of organobromide compounds in the marine environment. The mechanism takes place through bromination of different organic substrates like β diketones and β keto acids from the polypeptide pathway (Manley, 2002) (Figure 1.11).

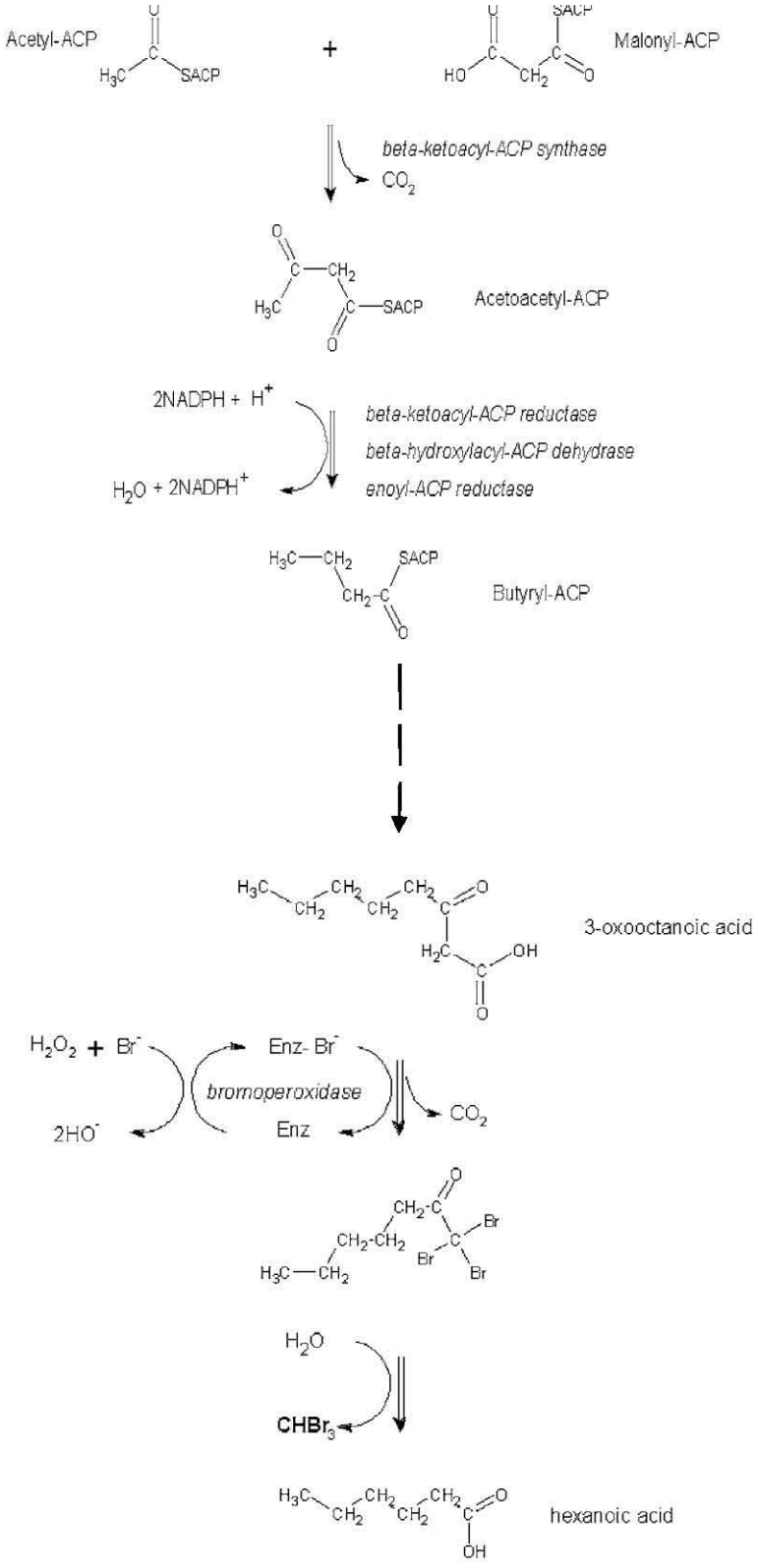

Figure 1.11: Biosynthesis of bromoform from β-keto acids adapted from Manley (2002)

Oxidation followed by substitution reaction of the compounds, result in unstable intermediate product (polybrominated ketone). Hydrolysis of the intermediate product(s) produces end products including bromoform (Manley, 2002). The whole process of bromoform production is regulated by the enzyme bromoperoxidase and, as such, its production depends on the mechanisms that influence bromoperoxidase activity.

1.6.1 Effects of light intensity

Bromoform production is considered to be impacted by light intensity (Figure 1.8) (Goodwin et al., 1997a). The observations therein can be linked to the fact that bromoform is a by-product of the activity of bromoperoxidase enzyme, which utilizes H_2O_2 as a substrate. H_2O_2 being one of the by-product of photosynthesis, it is mostly produced during the day. Experiments on macroalgae showed that the addition of a photosynthetic inhibitor (DCMU) to the organism lowered the production of bromoform (Figure 1.12) (Goodwin et al., 1997a; Manley and Barbero, 2001). The added chemical (DCMU) blocked the electron flows towards PSII which then inhibited photosynthesis and also limited H_2O_2 production (Manley, 2002).

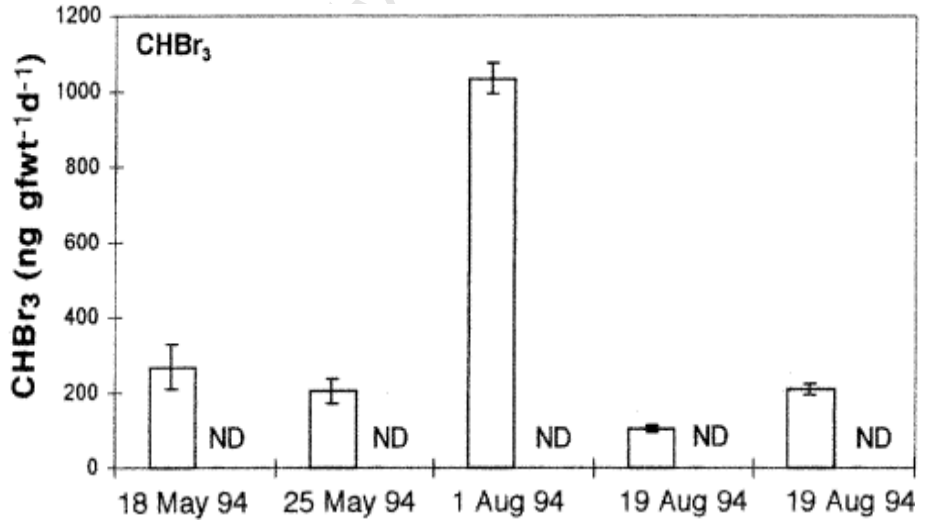

Figure 1.12: Production rates of bromoform for a macroalgae (*M. pyrifera*) (Goodwin et al., 1997a). The observed bars represent samples with non-DCMU and the ND (no detection of bromoform production) represent the samples with DCMU. Error bars are ±1 SE of regression.

1.6.2 Effects of nutrients

It is thought that a decrease in nutrients is linked to an increase in oxidative stress. It is known that under stress conditions *e.g.* high salinity and CO_2 limitation, the formation of ROS increases and as a result, oxidative stress increases (Noctor and Foyer, 1998; Sunda et al., 2002). Vardi et al. (1999) showed that a decrease in CO_2 concentration, both in the culture and natural environments, stimulated the formation of reactive oxygen species in cultured dinoflagellate *Peridium gatunene*. The accumulation of ROS, induced protoplast shrinkage and DNA fragmentation before cell death. Accumulation of reactive oxygen species will cause more anti-oxidant enzymes to be produced by the cell. Bucciarelli and Sunda (2003) observed an increase in the sulfur-containing anti-oxidant dimethyl-sulfoniopropionate (DMSP) as a result of decreasing nutrients (i.e. nitrate, phosphate and silicate) and CO_2 concentration in a cultured marine diatom.

A decrease in the concentration of nutrients at the surface of the ocean can result in increased bromoform production by algae. Krysell (1991) conducted a study on phytoplankton in the Arctic Ocean investigating the relationship between bromoform and nitrate concentration. An inverse relationship between the two was observed and it was concluded that nutrients like nitrate can control bromoform production. Because of global change, the input of nutrients to the surface waters of the ocean may be reduced due to an increase in stratification (Falkowski et al., 1998). In that case, oxidative stress in surface waters may increase, and that may affect bromoform production.

1.7 Aims and objectives

While the production of some organobromine compounds (*e.g.* methyl bromide) by marine microalgae has been the subject of previous studied (Scarratt and Moore, 1996; Scarratt and Moore, 1998; Tokarczyk and Moore, 1994), less work has been done relating to bromoform production. According to recent research (Moore et al., 1996; Colomb et al., 2008) it was revealed that certain species of microalgae have the capacity to produce bromoform. For example, the diatom species *Nitzschia arctica* and *Porosira glacialis* (Moore et al., 1996) and *Chaetoceros neogracile* (Colomb et al., 2008) have been observed to produce high

concentrations of bromoform. Diatoms are relatively large cells (diameter > ~5µm) which bloom when the flux of nutrients in the surface waters increases due to transient processes, such as upwelling events (Falkowski et al., 1998). These siliceous species contribute up to 40% of the global oceanic primary production of carbon (Nelson et al., 1995), and because of their wide repartition over the oceans, they might play a major role in bromoform production. Therefore, there is a need to conduct culture studies in order to quantify the production of bromoform by marine diatoms.

Most of the existing culture studies on bromoform production by phytoplankton were conducted with bacterial contamination (Moore et al., 1996; Colomb et al., 2008). Colomb et al. (2008) conducted studies on *Chaetoceros neogracile* and *Phaeodactylum tricornutum*, and showed their ability to produce bromoform. The production rates were 16 times greater (0.0016 pmol L^{-1}/Chl a)) in *Chaetoceros neogracile* than *Phaeodactylum tricornutum* (0.0001 pmol L^{-1}/Chl a). The experiments started with cultures under axenic conditions, but later the cultures became contaminated by ambient bacteria because of unsterilized equipment. Because bacteria also produce organobromine compounds (Goodwin et al., 1997b; Gribble, 2003), there is a need to conduct a study under axenicity to quantify the actual bromoform production by diatoms.

The link between bromoform production and oxidative stress on cultured marine diatoms has not yet been investigated, although several studies were conducted in nutrient rich cultures (Colomb et al., 2008; Moore et al., 1996). Other measurements were made during diatom senescence but there is no clear explanation of which nutrient is limiting (Tokarczyk and Moore, 1994); Moore et al., 1996). This provides a research opportunity to investigate which nutrient is limiting and can cause bromoform production as a result of increased oxidative stress.

The scientific objective for this project was: Quantifying axenic production of bromoform by diatoms and link with oxidative stress. To answer that objective the following was done

1. Determine the bromoform production in axenic cultures of *Chaetoceros neogracile* and *Phaeodactylum tricornutum* under carbon-dioxide limitation.

2. Determine the bromoform production in axenic cultures of *Phaeodactylum tricornutum* under nitrate limitation.

CHAPTER 2

MATERIAL AND METHODS

2.1 Model species

The diatom species used for this experiment were *Chaetoceros neogracile* and *Phaeodactylum tricornutum* (clone CCMP 1425 and 633 respectively). These species were chosen for this experiment because: i) It has already been proven that they produce bromoform (Colomb et al., 2008) and ii) The two strains were isolated from subtropical waters (CCMP 1425: 22N 72W Turtle Cove, Providenciales, Turks and Caicos Islands, British West Indies, CCMP 633: 14N 145E Territory of Guam (USA) Northern Mariana Islands) (http://ncma.bigelow.org/node/1/strain) where high fluxes of bromoform from the ocean into the marine atmosphere boundary layer (MABL) are measured (Yokouchi et al., 2005). *Chaetoceros neogracile* and *Phaeodactylum tricornutum* have different shapes (i.e. centric and pennate respectively) and size (i.e. 60-100 μm^3, as obtained in this study and 60-330 μm^3, according to the CCMP website respectively) (Figure 2.1).

a) **b)**

Figure 2.1: Scanning electron microscope image of *C. neogracile* (http://ncma.bigelow.org/node/1/strain/CCMP1425) (a) and *P. tricornutum* (http://www.sbs.utexas.edu) (b). *C. neogracile* is centric while *P. tricornutum* is pennate.

2.2 Culture conditions

The unialgal cultures were bought axenic (no bacterial contamination) from NCMA (formerly the CCMP) (https://ncma.bigelow.org). Batch cultures were conducted in 1-liter Duran® glass bottles at 21 ± 1^0C under saturating fluorescent continuous light (BioSun NL® -T858W/965; irradiance of 180 µmol photons m^{-2} s^{-1}). Both species were grown in f/2 medium (see below). The bottles were tightly sealed with PTFE seal caps (Colomb et al., 2008). This minimizes the exchange of gas (i.e. CO_2 and bromoform) with the atmosphere.

The transfers of the culture and medium preparation were done aseptically under a laminar flow hood. Ethanol was used to sterilize the laminar flow hood and the hands at any time of sampling. The laminar flow hood was used to maintain the axenicity of the culture by avoiding bacterial contamination from the air (Scarratt and Moore, 1996). In addition to that, all the equipment used for medium preparation and transfers of the culture was sterilized by autoclaving or bought sterile. The culture axenicity was checked regularly by pipetting ~1 mL of cultures into ~5 mL of sterile bactopeptone media (1 g L^{-1}). The absence of bacteria growth was confirmed after 7 days at room temperature in the dark. Before sampling the culture were gently mixed by ~50 reversals (Bucciarelli et al., 2007).

2.3 Culture medium

The complete medium consisted of 0.2 µm filtered False Bay seawater enriched with nutrients (f/2 medium) (Guillard, 1975). The initial concentration of macro-nutrients in sea water was 5.4 ± 1.5 µM (n=5) of nitrate (NO_3^-), 0.5 ± 0.4 µM (n=5) of phosphate (PO_4^{3-}) and 8.6 ± 1.0 µM (n=5) of silicate (SiO_4^-). Concentrations of macro-nutrients, trace metals and vitamins in the media are shown in table 2.1.

Table 2.1: Concentrations of macronutrients, trace metals and vitamins in f/2 medium

Component		Molar concentration
Macronutrients	N	8.82×10^{-4} M
	P	3.62×10^{-5} M
	Si	1.06×10^{-4} M
Trace metals	Fe	1.17×10^{-5} M
	EDTA	1.17×10^{-5} M
	Cu	3.93×10^{-8} M
	Mo	2.60×10^{-8} M
	Zn	7.65×10^{-8} M
	Co	4.20×10^{-8} M
	Mn	9.10×10^{-7}M
Vitamins	B_1	2.96×10^{-7} M
	H	2.05×10^{-9} M
	B_{12}	3.69×10^{-10} M

Prior to the addition of macronutrients, trace metals and vitamins, 0.2 µm filtered sea water was sterilized in 1 Liter bottles by microwave for 8 minutes (Keller et al., 1988). However, boiling of sea water by microwave increases pH (from ~8.0 to ~8.3) because of outgassing of CO_2. Lowering pH back to ~7.8 was achieved by addition of hydrochloric acid (HCl) and buffered by sodium hydrogeno carbonate ($NaHCO_3$). Lowering of pH helps to avoid CO_2 limitation at an early stage of the culture growth.

2.4 Types of experiments

When the experiments began, the cultures were first grown to adapt to their environment for at least 10 generations. After that, the cultures were grown for a preliminary experiment to measure cellular parameters (*e.g.* maximum cell concentration and growth rate) and estimates of macronutrient assimilation (Annex: Table1a and b).

Two main experiments were conducted under semi-continuous conditions. This was done by diluting the cultures with fresh medium after sampling (Sunda et al., 2002). All the data obtained from these experiments were corrected from dilution effects. During the main experiments, three culture phases were studied: 1) Exponential phase (2 experiments for *C. neogracile* and *P. tricornutum*), 2) CO_2

limited growth (1 experiment for *C. neogracile* and *P. tricornutum*), and 3) NO_3^- limited growth (1 experiment for *P. tricornutum*) (Figure 2.2). Exponential phase 1 and CO_2 limitation experiments were conducted in triplicates. Exponential phase 2 and NO_3^- limitation experiments were conducted in duplicates.

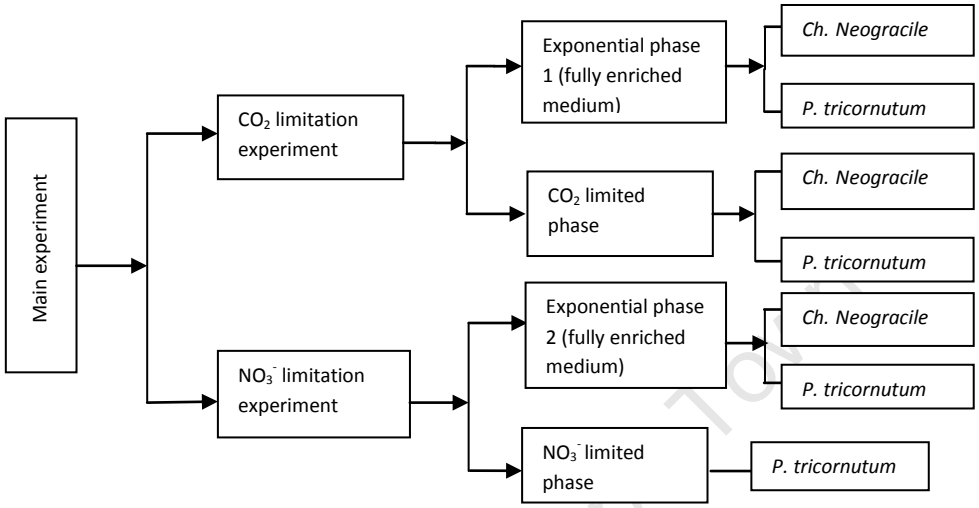

Figure 2.2: Scheme of the main experiments

Collection of samples during the main experiments is described in figure 2.3.

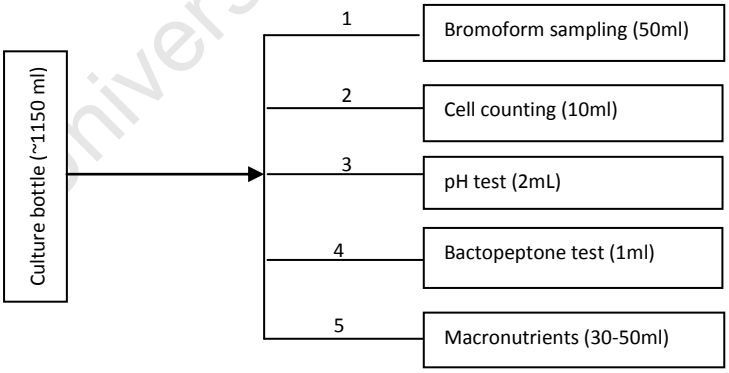

Figure 2.3: Procedure used to collect samples from culture bottles

To avoid head space and loss of bromoform in the gas phase, cultures were refilled with new medium immediately after sampling (Bucciarelli et al., 2007). Refilling was done using the same medium as for the cultures. Control bottles

consisted of medium without diatoms. The controls were kept in identical conditions as the cultures (Moore et al., 1996, Colomb et al., 2008). For the control only bromoform, pH and bactopeptone were sampled.

At the end of exponential phase 1, cultures were forced to CO_2 limitation. Addition of NaOH (5M) increased pH to 9.0 ± 0.1 and this ensured that cultures entered CO_2 limitation (Sunda et al., 2002). To make sure the cultures are only limited with CO_2, macronutrients were added each day after sampling. The amount of macronutrient added was based on the calculations drawn from the preliminary experiment.

Limitation of cultures by nitrate was achieved by allowing cultures to grow without addition of nitrate. Phosphate and silicate were added after each sampling and pH was maintained below 8.3 by adding saturated $NaHCO_3$ and concentrated HCl.

2.5 Sampling and analysis of the cellular parameters

Sampling for cell concentration (for *C. neogracile* and *P. tricornutum*) and volume per cell (for *C. neogracile*) was conducted once every day until the end of the experiment as described by Bucciarelli and Sunda (2003). Within 20 minutes of sampling for each bottle, cell abundance per liter of culture (C_{cell}, L^{-1}_{medium}) and volume per cell (V_{cell}, μm^3) was measured using a 2-2 Multisizer Coulter Counter analyzer. The aperture size used was 100 µm and the range of the particle size was 20-150 μm^3. Measuring volume per cell using a coulter counter works only for spherical particles. For this experiment the volume per cell was measured for *C. neogracile* (centric diatom) but could not be measured for *P. tricornutum* (pennate diatom). The specific growth rate (μ, d^{-1}) was calculated by dividing the natural logarithm of cell abundance per liter of culture (C_{cell}, L^{-1}_{medium}) by time (day(s)) between samplings (Sunda and Huntsman, 1995) according to Equation (2.5-1):

$$\mu = \frac{(\ln N_2) - (\ln N_1)}{(t_2 - t_1)} \qquad (2.5\text{-}1)$$

2.6 Nutrients sampling and analysis

2.6.1 pH: The pH of the cultures was monitored throughout the experiment using a HANNA model (HI 9125) pH/ORP meter. For each sample, the measurement of pH (at room temperature) was done within ~10 minutes after sampling. Measuring pH was used as an index of carbon limitation (Scarratt and Moore, 1996). When the pH reaches ≥ 8.5, carbon limitation may occur (Goldman et al., 1982).

2.6.2 Macronutrients*:* Sampling for macronutrients (nitrate, phosphate and silicate) was conducted once every day until the end of the experiments. Cultures were filtered using 25 ml disposable syringe and 0.2 µm disposable filters for nitrate, phosphate and silicate measurements. 50 mL plastic bottles were used for storing samples. The samples were then kept in the fridge for ~3 weeks. The concentration of nitrate, phosphate and silicate was measured colorimetrically.

2.6.2.1 Nitrate: Nitrate was determined following the protocol described by Strickland and Parsons (1965). Nitrate in the sample is determined by reduction to nitrite. In a basic solution the reduction proceeds according to the following equation.

$$NO_3^- + H_2O + 2e^- \longrightarrow NO_2^- + 2OH^-$$

The reduction is done by passing the samples through a column of copperized cadmium granules. The column is treated with alkaline ammonium chloride solution to complex the oxidized Cd^{++} ions, thus prolonging the life of the column. The column decreases in efficiency with use because of the formation of $Cd(OH)_2$. Nitrite is determined by diazotization with sulphanilimide, and then coupled with N-(1-naptyhyl)-ethylene diamine hydrochloride to produce a red color (Bendschneider and Robinson, 1952). Absorbance is determined within 2 hours with a spectrophotometer at a wavelength of 540 nm. The concentration of nitrite was determined thanks to a calibration curve of seven standards (Figure 2.4).

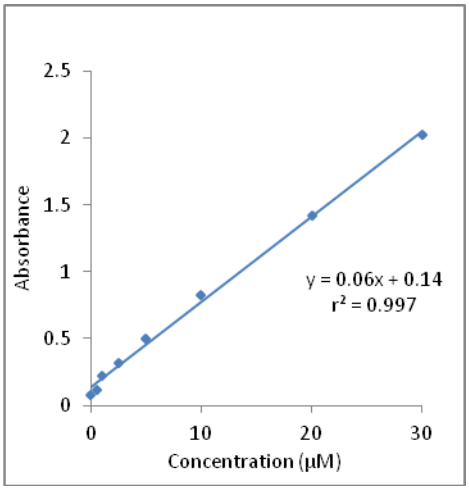

Figure 2.4: Calibration curve of seven nitrite standards

The reduction efficiency was determined by comparing the corrected absorbance, of a nitrite standard slope with the corrected absorbance of a reduced nitrate standard slope.

An aliquot of the sample was first analyzed without using the reduction step, to measure the initial concentration of nitrite, $NO_{2\ init}^-$. Then, a second aliquot was passed through the cadmium column to reduce nitrate to nitrite, and analyzed. This second analysis gives a concentration of nitrite resulting from the initial nitrite concentration in the sample, $NO_{2\ init,}^-$ plus the nitrate concentration in the sample that has been reduced to nitrite by the Cd column, NO_3^-.The concentration of nitrate was then calculated by substracting the concentration measured during the first analysis ($NO_{2\ init,}^-$) to the concentration measured during the second analysis ($NO_{2\ init}^- + NO_3^-$).

2.6.2.2 Phosphate: Phosphate was determined following the protocol described by Greenfield and Kalber (1954) and Murphy and Riley (1958). The method uses a single reagent containing ammonium molybdate, ascorbic acid, sulphuric acid and potassium antimony tetrate. The orthophosphate ions in the samples react with ammonium molybdate and potassium antimony tetrate under acidic conditions and form a yellow complex. Ascorbic acid is used to reduce the complex. Absorbance is determined within 10 minutes to 1 hour with a spectrophotometer

at a wavelength of 880 nm. The concentration of phosphate was determined thanks to a calibration curve of nine standards (Figure 2.5).

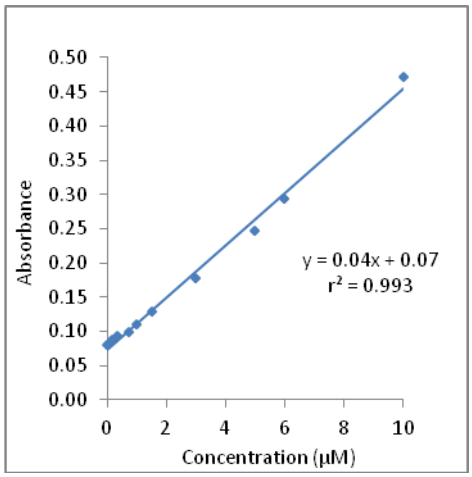

Figure 2.5: Calibration curve of nine phosphate standards

2.6.2.3 Silicate: Silicate was determined following the method described by Dienért and Wandenbulcke (1923). The method makes use of the yellow color of the silicomolybdic acid which is formed when ammonium molybdate and sulphuric acid are added to the sample. The complex is subsequently reduced with ascorbic acid to form a blue complex which has an absorbance maximum at 810 nm. The color is then compared with that of standard made up of silicofluoride (Figure 2.6).

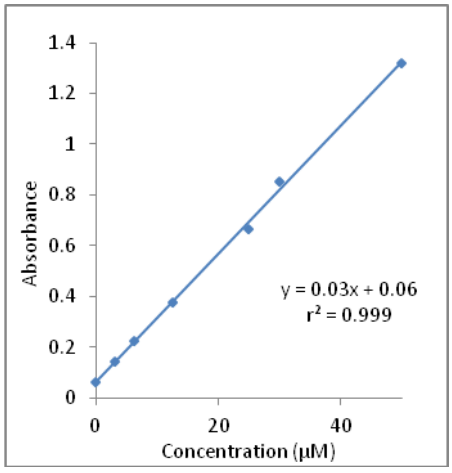

Figure 2.6: Calibration curve of silicate standards

2.7 Bromoform sampling and analysis

Bromoform measurement was carried out using Electron Capture Detector (ECD) Gas Chromatography (GC) which has been built in house, together with thermal desorption cooled adsorbent trap (Palmer et al., *In Prep*). Unfiltered samples were collected into cold trap glass bottle with a purge tube (Moore et al., 1996). The tube was connected to 5 grade nitrogen (ultrapure-nitrogen) to purge the samples for 5 minutes at 20°C. The flow rate of nitrogen was regulated by means of a porter valve. Bromoform was trapped into an adsorbent trap at room temperature. The removal of water vapor from the trap system was done by allowing nitrogen to flow for about 2 minutes (Moore et al., 1996). The peak identifications from gas chromatography were achieved by comparing the results with known standards (Manley et al., 1992). To avoid contamination of samples in the detector, samples of laboratory MQ water were analyzed at the beginning and the end of each day session and in between samples (Moore et al., 1996).

Bromoform standards were analyzed by following the same procedure as the samples. The first standard was prepared using pure bromoform diluted into methanol (85 µL of 98% bromoform was first diluted into 100 mL of methanol). Then the second standard was made by diluting the first standard into methanol (85 µL of the first standard diluted into 110 mL of methanol). The standards used for the calibration were then all made using the second standard mixed volumetrically into f/2 medium (Moore et al., 1996). Analysis of the standards by the GC gave us the bromoform peak areas which were used to draw a calibration curve (Figure 2.7).

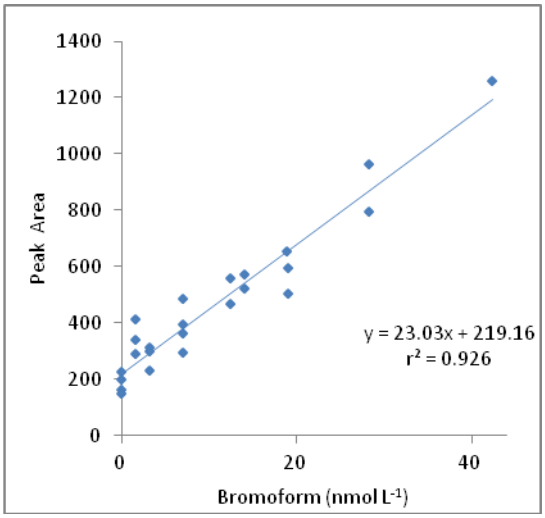

Figure 2.7: Calibration curve of bromoform standards

Bromoform was also measured in the control bottles. Using figure 2.7 the concentration of bromoform in the cultures was calculated based on the following equation:

$$\text{concentration} = \frac{(\text{peak area})\text{culture} - (\text{peak area})\text{control}}{\text{slope}}$$

Where slope = 23.03 (from figure 2.7)

Although bromoform is in the dissolved phase (i.e. not intracellular), the concentration was calculated relative to cell concentration and cell volume for comparison's sake between samples.

CHAPTER 3

RESULTS

The results are presented into the following subsections:

i) Preliminary experiment,

ii) Exponential phases 1 and 2,

iii) Carbon dioxide (CO_2) limitation experiment,

iv) Nitrate (NO_3^-) limitation experiment.

3.1 Preliminary experiment

3.1.1 Specific growth rates

Both *P. tricornutum* and *C. neogracile* showed exponential changes of cell concentrations with time during the exponential growth (Figure 3.1a and b).

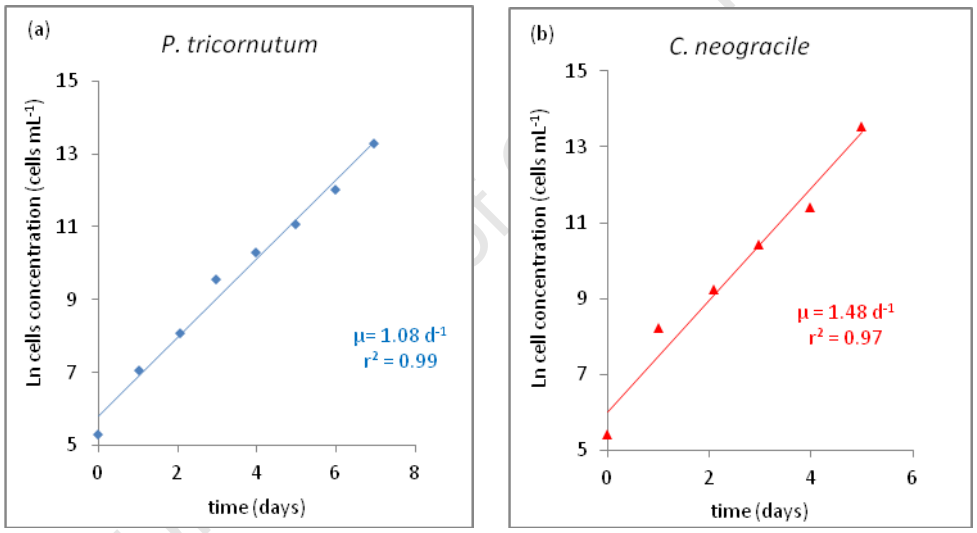

Figure 3.1: Change of natural log of cell concentration (cells mL^{-1}) with time (days) for *P. tricornutum* (a) and *C. neogracile* (b). Slopes give the specific growth rates (μ, d^{-1}).

The change of cell concentration for *P. tricornutum* was from 202 cells mL^{-1} to 585004 cells mL^{-1} between day 0 and day 7 of the incubation. The average specific growth rate obtained was μ=1.08 d^{-1} (r^2=0.99, n=8). The same strain of *P. tricornutum* (CCMP 633) grows at 0.42 to 0.54 d^{-1} in artificial sea water, under 12:12 light: dark cycle at 19°C and 60-80 µmol m^{-2} s^{-1} (Martino et al., 2007). The

difference of growth rate between this study and that by Martino et al. (2007) might be caused by differences in culture conditions.

For *C. neogracile* cell concentration changed from 228 cells mL^{-1} to 765170 cells mL^{-1} between day 0 and day 5. The average specific growth rate obtained was $\mu=1.48\ d^{-1}$ ($r^2=0.97$, n=6). The few other studies on the same strain of *C. neogracile* (*e.g.* Colomb et al., 2008) did not present the growth curve or the specific growth rate. The maximum growth rate of another strain of *C. neogracile* (CCMP 1317) from subtropical waters is 0.78 d^{-1} (Cuesta and Manley 2009).

Besides, according to the comprehensive review by Eppley (1972) and that of Banse (1982), the maximum growth rate of small diatoms (60-100 μm^{-3}) at 20°C ranges between 1.8 and 3.2 d^{-1}. Sarthou et al. (2005) also reviewed different culture studies of diatoms. Based on their analysis, the maximum growth rate of diatoms under saturating light and sufficient nutrients ranges from 0.4 to 3.3 d^{-1} with a value of ~1.9 to 2.0 d^{-1} for a cell volume between 60 to 100 μm^3, and ~1.6 to 2.0 d^{-1} for a cell volume between 60 to 330 μm^3. The growth rates of *C. neogracile* and *P. tricornutum,* whose volume ranged between 56-98 μm^3 and 60-330 μm^3 respectively in this study, are within the same order of magnitude.

3.1.2 Assimilation of macronutrients

During the exponential growth, *P. tricornutum* and *C. neogracile* assimilate nutrients (Figure 3.2).

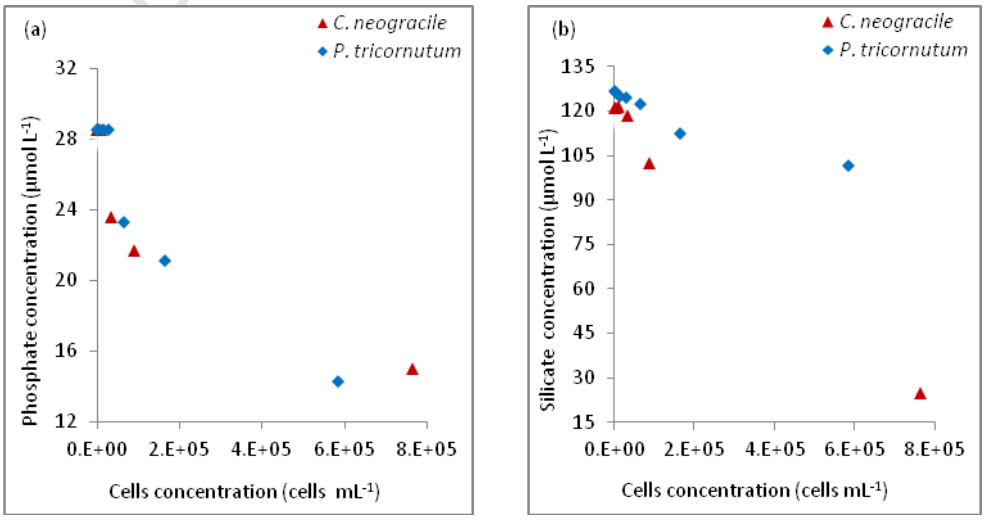

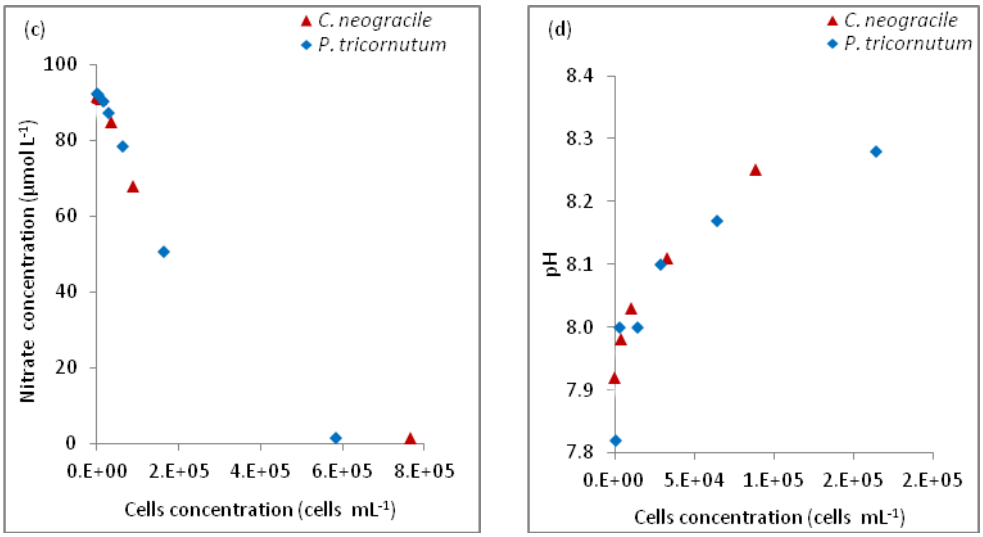

Figure 3.2: Change of macronutrients (µmol L^{-1}) with cell concentration (cells mL^{-1}) for *P. tricornutum* (diamonds) and *C. neogracile* (triangles). (a) represents phosphate, (b) silicate, and (c) nitrate. (d) Shows change of pH with cell concentration.

Nutrient assimilation per cell was calculated by using the following equation:

$$\text{nutrient consumption } (\text{mol cell}^{-1}) = \frac{Cn_1 - Cn_2}{N_2 - N_1}$$

Where: Cn_1 = nutrients concentration at t_1 (µmol L^{-1})

Cn_2 = nutrients concentration at t_2 (µmol L^{-1})

N_1 = Cell concentration at t_1 (cells mL^{-1})

N_2 = Cell concentration at t_2 (cells mL^{-1})

The equation was applied at 3 different points i.e. from day 4 to 6 for *P. tricornutum* and day 2 to 4 for *C. neogracile*. During these days, the change of cell concentrations and macronutrients was significant.

The mean and standard deviation of nutrient assimilation per cell for these data points are presented in table 3.1.

Table 3.1: Mean ± STD of macronutrient per cell (*f*mol cell^{-1}) for *P. tricornutum* and *C. neogracile* during the preliminary experiment.

	P. tricornutum	*C. neogracile*
Concentration (*f*mol cell^{-1})	Mean ± STD	Mean ± STD
Nitrate	175 ± 23	289 ± 22
Phosphate	90 ± 35	128 ± 41
Silicate	80 ± 30	208 ± 96

The nutrient assimilation per volume of cell was calculated using the equation below:

$$\text{nutrient assimilation } (\text{mol } \mu\text{m}^{-3}) = \frac{Cn_1 - Cn_2}{CV_2 - CV_1}$$

Where; Cn_1 = nutrients concentration at t_1 (µmol L^{-1})

Cn_2 = nutrients concentration at t_2 (µmol L^{-1})

CV_1 = Total cell volume at t_1 (μL_{cell} L^{-1})

CV_2 = Total cell volume at t_2 (μL_{cell} L^{-1})

Since *C. neogracile* is centric, its volume was obtained directly from the coulter counter. The total cell volume of *C. neogracile* was measured each day (Annex: Table 1 b). For *P. tricornutum,* which is pennate, the volume was calculated based on equation (3.1B-1) (Bartual et al., 2008):

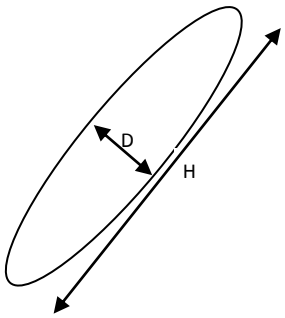

$$V_T = \frac{\pi}{6} D^2 H \qquad (3.1B\text{-}1)$$

The mean diameter (D) and Length (H) of this strain was 3-5 µm and 13–25 µm respectively, according to the CCMP website where the strain has been purchased

(http://ncma.bigelow.org/node/1/strain). By using equation (3.1B-1), calculated cell volume of *P. tricornutum* ranges from 60 to 330 μm^3. This range of cell volume is used to calculate total cell volume for each day (Annex: Table1a).

The nutrient assimilation per volume of cell is presented in table 3.2

Table 3.2: Macronutrient per cell volume (*f*mol μm^{-3}) for *P. tricornutum* and *C. neogracile*

	P. tricornutum		*C. neogracile*
	Lower range	Upper range	
Concentration (*f*mol μm^{-3})	Mean ± STD	Mean ± STD	Mean ± STD
Nitrate	(0.8 ± 0.1)	- (4.4 ± 0.5)	3.1 ± 0.1
Phosphate	(0.3 ± 0.1)	- (1.5 ± 0.8)	1.8 ± 0.9
Silicate	(0.3 ± 0.1)	- (1.3 ± 0.4)	2.8 ± 1.2

3.1.3 Change in pH

pH ranged from 8.00 to 8.28 for *P. tricornutum* and from 7.98 to 8.25 for *C. neogracile* (Figure 3.2d; Annex: Table1a and b). Based on the study by Goldman et al. (1982), diatoms start to experience carbon limitation at pH ≥ 8.5, which results in the decline of growth rate and photosynthesis. The effects of pH increase on the growth of *Thalassiosira pseudonana* and *Thalassiosira ocenica* was observed by Chen and Durbin (1994). Their culture pH ranged from 7.0 to 9.4. At pH ≥ 8.8, consistent declines of growth rate and photosynthesis were observed. The range observed in our study is favourable for maximum cell growth.

These estimates of changes in macronutrients (phosphate, silicate, and nitrate) and pH versus cell concentration, calculated from the preliminary experiments, were used in the following experiments to ensure that the cells did not experience any limitation during the exponential phase and experienced only CO_2 or nitrate limitation during the limited phase. To do so, 0.2 µm filtered solution of nitrate, phosphate, silicate and/or $NaHCO_3$ were added to the growing cultures when needed, according to the cell concentration measured each day.

3.2 Exponential phase 1 and 2

The minimum and maximum concentrations of macronutrients and pH values during exponential phases are shown in table 3.3

Table 3.3: Minimum and maximum concentrations of macronutrients (µmol L^{-1}) and pH values in the cultures of *P. tricornutum* and *C. neogracile* during exponential phase 1 and 2.

	Exponential phase1		Exponential phase2	
	P. tricornutum	*C. neogracile*	*P. tricornutum*	*C. neogracile*
Nitrate (µmol L^{-1})	596 - 745	715 - 841	253 - 858	603 - 760
Phosphate (µmol L^{-1})	23 - 31	22 - 29	23 - 46	29 - 52
Silicate (µmol L^{-1})	110 - 132	75 - 129	127 - 182	139 - 233
pH	7.9 - 8.3	7.8 - 8.5	8.0 - 8.3	8.0 - 8.3

These values of macronutrients and pH show that the cultures were not limited and could experience maximum growth. More details on the macronutrient variations of each day are presented in annex (Table2a and b for exponential phase1; Table3a and b for exponential phase2)

The average specific growth rates for *P. tricornutum* and *C. neogracile* during exponential phase 1 are reported in figure 3.3a and b.

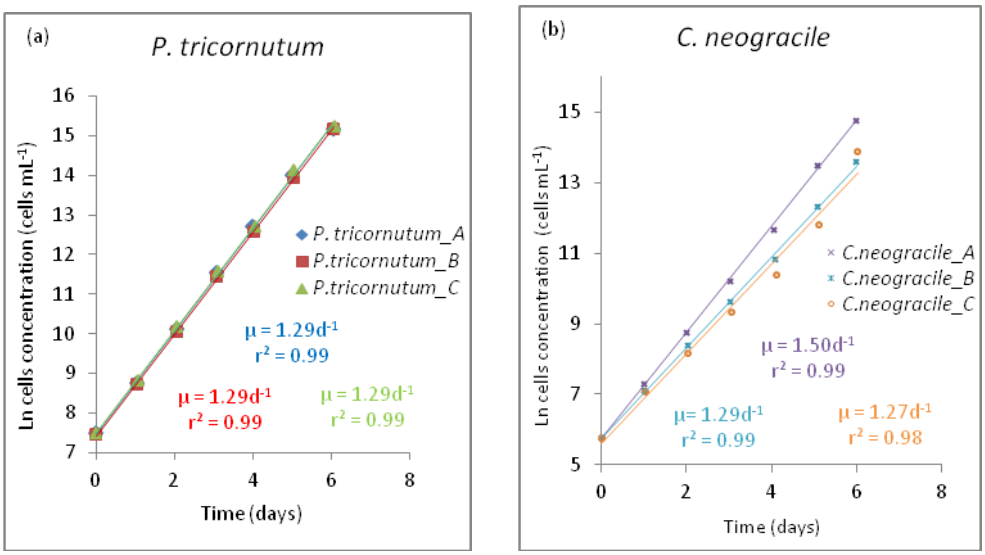

Figure 3.3: Change of natural log of cell concentration (cells mL^{-1}) with time (days) for *P. tricornutum* (a) and *C. neogracile* (b) in triplicates (A, B and C) during exponential phase1. Slopes give the specific growth rates.

Specific growth rate of *P. tricornutum* during exponential phase1 was the same in all triplicates with an average of 1.29 ± 0.00 d^{-1} (n=3) (Mean ± SD). For *C. neogracile,* the growth rate ranged from 1.27 to 1.50 d^{-1} with an average growth rate of 1.35 ± 0.13 d^{-1} (n=3).

During exponential phase 2, *P. tricornutum* and *C. neogracile* were grown as duplicates (Figure 3.4a and b).

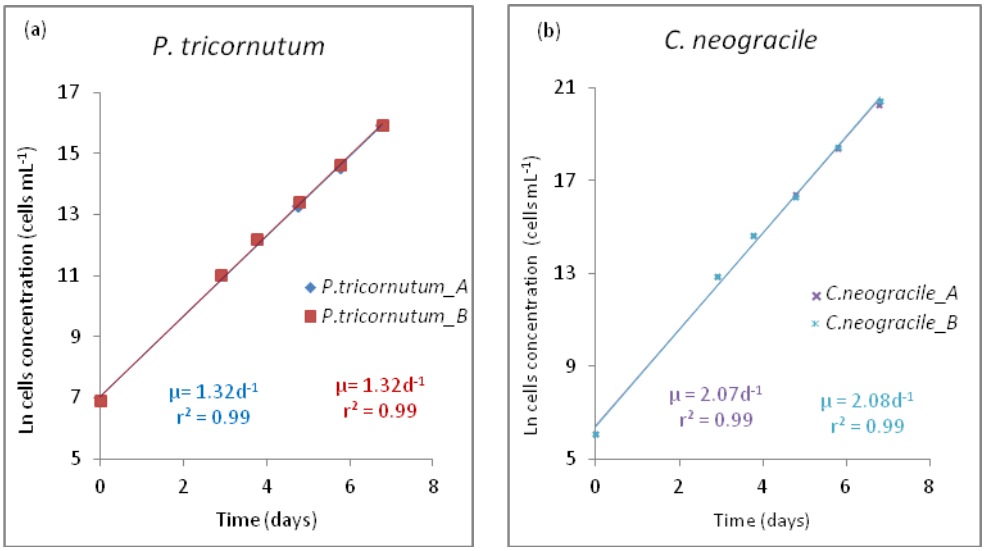

Figure 3.4: Change of natural log of cell concentration (cells mL^{-1}) with time (days) for *P. tricornutum* (a) and *C. neogracile* (b) in duplicates (A and B) during exponential phase 2. Slopes give the specific growth rates.

During exponential phase 2, the specific growth rate of *P. tricornutum* was the same between the duplicates: 1.32 ± 0.00 d^{-1} (n=2). The specific growth rate of *C. neogracile* was also similar between replicate A and B: 2.08 ± 0.00 d^{-1} (n=2).

When comparing the two exponential phases, *P. tricornutum* had approximately similar specific growth rates, with an average growth rate of 1.30 ± 0.02 d^{-1} (n=5). Differences in growth rate however existed for *C. neogracile* between exponential phase 1 and 2. Averaged specific growth rate for *C. neogracile* during exponential phase 1 was 1.35 ± 0.13 d^{-1} (n=3) while during exponential phase 2 it was 2.08 ± 0.01 d^{-1} (n=2).

Bromoform production by the cultures was measured during exponential phase 1 and 2 (data combined). Bromoform per cell (mol $cell^{-1}$) is presented in table 3.4.

Table 3.4: Bromoform per cell (x10^{-18} mol $cell^{-1}$) of *P. tricornutum* and *C. neogracile* during exponential phases 1 and 2 (data combined)

Concentration (x10^{-18}mol $cell^{-1}$)	*P. tricornutum*	*C. neogracile*
Range	5.3 - 12.4	4.4 - 40.7
Mean	9.0	16.5
STD	2.7	3.8
n	5	5

Average bromoform per cell was 9.0 ± 2.7 x 10^{-18} mol $cell^{-1}$ for *P. tricornutum* and 16.5 ± 3.8 x 10^{-18} mol $cell^{-1}$ for *C. neogracile*. Production of bromoform between the two species was not significantly different (t-test, p>0.1). Moore et al. (1996) measured bromoform concentrations in cultures of *Nitzschia sp.* and *Posira glacialis*. They also presented the growth curves which allow to extract the cell concentration for each bromoform data and to calculate a value of bromoform per cell. During exponential phase, average bromoform per cell for *Nitzschia sp.* is 18.9 x 10^{-18} mol $cell^{-1}$ and for *Posira glacialis* is 58.5 x 10^{-18} mol $cell^{-1}$. Measured bromoform per cell (mol$cell^{-1}$) for *P. tricornutum and C. neogracile* are in the same order of magnitude as those of *Nitzschia sp.* and *Posira glacialis.*

The bromoform production rate is calculated by multiplying the bromoform per cell by the specific growth rate (Table 3.5).

Table 3.5: Rate of bromoform production per cell (x10^{-18} mol $cell^{-1}d^{-1}$) of *P. tricornutum* and *C. neogracile* culture samples during exponential phases.

Bromoform production rate (x10^{-18}mol $cell^{-1}d^{-1}$)	*P. tricornutum*	*C. neogracile*
Range	7.0 - 15.6	8.5 - 57.0
Mean	11.4	28.0
STD	3.4	5.3
n	5	5

P. tricornutum and C. neogracile produced bromoform at different rates (Table 3.6). During the exponential phases, *C. neogracile* produced ~3 times more bromoform per cell per day than *P. tricornutum.* The differences in production

rates between the two species was significant (paired t-test, $p<0.05$). Colomb et al. (2008) also observed a higher production of bromoform by *C.* neogracile (about 16 times more) than by P. tricornutum. The average bromoform per cell per day measured by Moore et al. (1996) was 1.9 x 10^{-18} mol $cell^{-1}d^{-1}$ and 7.0 x 10^{-18} mol $cell^{-1}d^{-1}$ for *Nitzschia sp.* and *Posira glacialis* respectively as calculated by using their growth curves and inferring the specific growth rate for their species during exponential growth. *Nitzschia sp.* and *Posira glacialis* have lower rates of bromoform production compared to *P. tricornutum and C. neogracile* because they have lower growth rates.

3.3 Carbon dioxide (CO_2) limitation experiment

CO_2 limitation experiments were conducted following exponential phase 1. Limitation was induced at day 5 by adding NaOH in the cultures (see Material and Methods). CO_2 limitation was confirmed by the increase in pH (Figure 3.5)

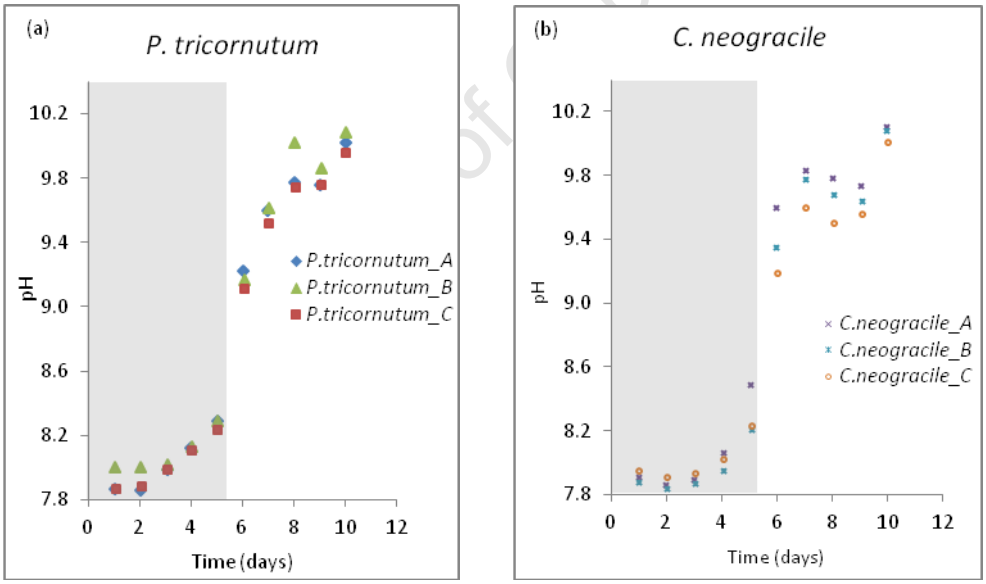

Figure 3.5: Change of pH with time (days) for *P .tricornutum* (a) and *C. neogracile* (b). Both cultures were in triplicate samples (A, B, and C). Shaded area represent exponential growth phase.

Between days 1 to 5 (shaded area), the pH ranged between 7.91 and 8.27 for *P. tricornutum* and 7.91 and 8.31 for *C. neogracile*. Although the pH increased with

time from day 1 to 5, that range is still appropriate for maximum culture growth (Goldman et al., 1982; Chen and Durbin, 1994). After addition of NaOH the pH increased to 9.17 ± 0.06 for *P. tricornutum* and 9.38 ± 0.21 for *C. neogracile* on day 6. This ensured that cultures were in CO_2 limitation. After inducing CO_2 limitation, the cultures were allowed to grow from day 6 to day 10 (un-shaded area). Throughout those days, the pH of the cultures still increased (Figure 3.5). The other nutrients (phosphate, silicate and nitrate) were added so that their concentrations were never limiting (Annex: Table 4a and b). The minimum and maximum concentrations of macronutrients during CO_2 limitation are shown in table 3.6.

Table 3.6: The minimum and maximum concentration of macronutrients (µmol L^{-1}) in the cultures of *P. tricornutum* and *C. neogracile* during CO_2 limitation

Concentration (µmol L^{-1})	*P. tricornutum*	*C. neogracile*
Nitrate	366 - 760	482 - 884
Phosphate	5 - 31	14 - 29
Silicate	91 - 181	59 - 330

During CO_2 limitation, the averaged specific growth rate was calculated between day 7 and 10 (Figure 3.6a and b).

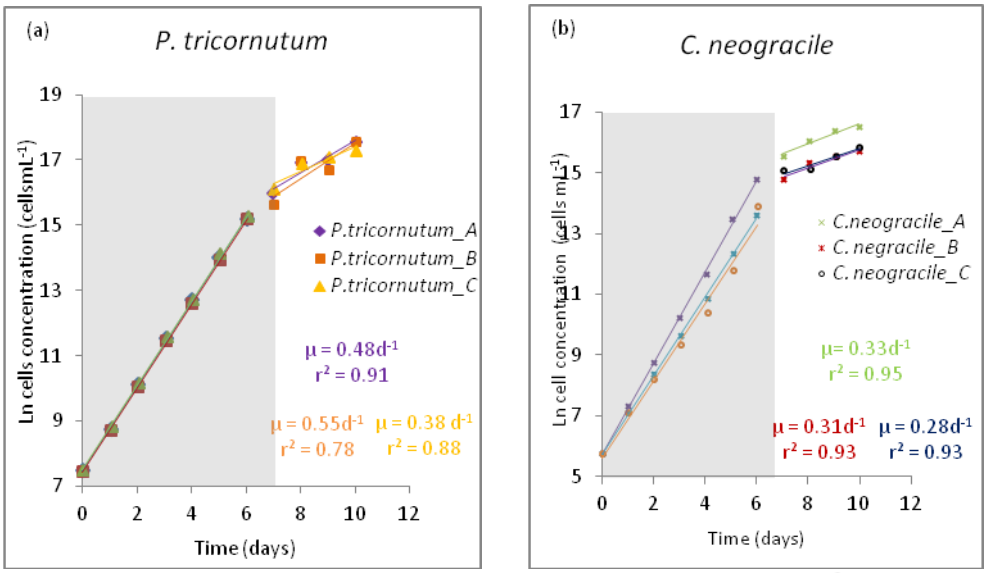

Figure 3.6: Change of natural log of cell concentration (cells mL^{-1}) with time (days) for *P. tricornutum* (a) and *C. neogracile* (b) in triplicates (A, B and C) during exponential phase1 (day 1 to 6, shaded area) and CO_2 limitation (day 7 to 10, un-shaded area). Slopes (between days 7 to 10) give the specific growth rates during CO_2 limitation.

During CO_2 limitation, the specific growth rate decreased (un-shaded area of figure 3.6a and b). The mean specific growth rates for *P. tricornutum* and *C. neogracile* were 0.56 ± 0.04 d^{-1} (n=3) (Mean ± SD) and 0.46 ± 0.04 d^{-1} (n=3) respectively. The specific growth rate during CO_2 limitation was 2.4 and 4.5 times lower for *P. tricornutum* and *C. neogracile* respectively, compared to their exponential phases.

The cultures produced bromoform during CO_2 limitation (Table 3.7 and 3.8).

Table 3.7: Bromoform per cell (x10^{-18} mol $cell^{-1}$) of *P. tricornutum* and *C. neogracile* during CO_2 limitation

Bromoform per cell (x10^{-18}mol $cell^{-1}$)	*P. tricornutum*	*C. neogracile*
Range	1.7 - 6.6	1.8 - 3.6
Mean	4.0	3.1
STD	0.4	0.2
n	5	5

Table 3.8: Rate of bromoform production (x10^{-18} mol $cell^{-1}d^{-1}$) of *P. tricornutum* and *C. neogracile* during CO_2 limitation

Bromoform per cell per day (x10^{-18}mol $cell^{-1}d^{-1}$)	*P. tricornutum*	*C. neogracile*
Range	0.0 - 5.6	0.4 - 1.8
Mean	2.6	1.3
STD	0.9	0.2
n	5	5

Average bromoform per cell was 4.0 ± 0.4 x 10^{-18} mol $cell^{-1}$ for *P. tricornutum* and 3.1 ± 0.2 x 10^{-18} mol $cell^{-1}$ for *C. neogracile* (Table 3.7), which was not significantly different (t-test, p>0.1).The mean rate of bromoform per cell (mol $cell^{-1}d^{-1}$) was not significantly different between the two species either (t-test, p=0.1).

3.4 Nitrate (NO_3) limitation experiment

The NO_3 limitation experiment for *P. tricornutum* was conducted following exponential phase 2. From the initial concentration of nitrate (859 µmol L^{-1} for sample A and 734 µmol L^{-1} for sample B) the cultures were allowed to grow for about 12 days without further addition of nitrate (Figure 3.7).

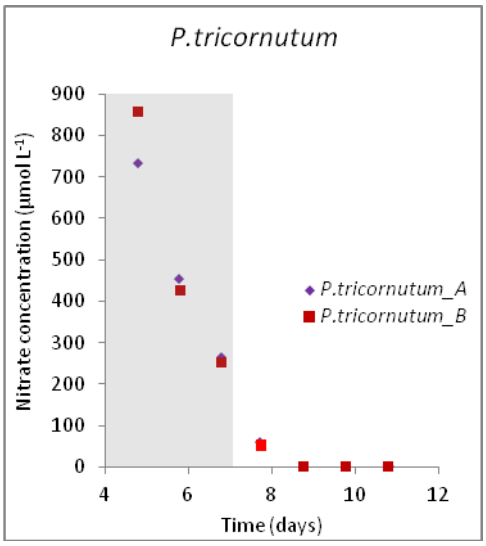

Figure 3.7: Change of nitrate (µmol L^{-1}) with time (days) for *P. tricornutum.* Sample A (diamonds) and sample B (rectangle).

After day 8 (Figure 3.7) the nitrate in the culture was at its lowest concentration. This ensured the cultures were nitrate limited from day 9. Throughout the experiment, the other nutrients (phosphate, silicate and CO_2) were at concentrations high enough for maximum culture growth (Annex: Table5). The minimum and maximum concentrations of phosphate, silicate and pH during NO_3 limitation are shown in table 3.9.

Table 3.9: The minimum and maximum of phosphate (µmol L^{-1}), silicate (µmol L^{-1}) and pH values in the cultures of *P. tricornutum* during NO_3^- limitation

	P. tricornutum
Phosphate (µmol L-1)	66 - 121
Silicate (µmol L-1)	253 - 413
pH	8.05 - 8.26

When the cultures became depleted with nitrate, the growth rate decreased (Figure 3.8).

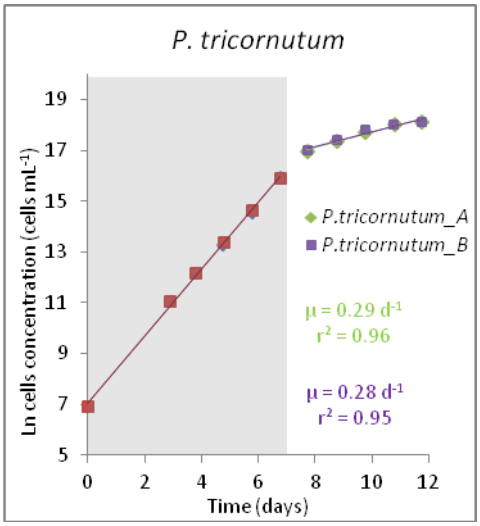

Figure 3.8: Change of natural log of cell concentration (cells mL^{-1}) with time (days) for *P. tricornutum* in duplicate. Sample A (diamonds) and sample B (rectangles). Slopes of un-shaded area, gives the specific growth rates during NO_3^- limitation.

During nitrate limitation, the averaged specific growth rate calculated between day 8 and 12 (Un-shaded region of figure 3.8) was 0.30 d^{-1} (replicate A) and 0.28 d^{-1} (replicate B). The growth rate of *P. tricornutum* during NO_3^- limitation was about 5 times lower than the maximum growth rate during exponential phase.

During nitrate limitation, the bromoform concentrations in the cultures never exceeded the control values (i.e. 7.0 ± 0.8 nmol L^{-1}; n=5 for cultures and 9.3 ± 0.8 nmol L^{-1}; n=5 for blanks). This suggests that no bromoform was produced by the nitrate limited cells.

CHAPTER 4

DISCUSSION

The variation in the specific growth rate of the species between the exponential phase and the limited phase is first discussed. This variability is then related to the concentrations of bromoform measured in the cultures and, based on existing literatures, different hypotheses are proposed to explain the link between diatom growth and bromoform production.

4.1 Variations of growth rates from the exponential phase to the limited phase

4.1.1 During exponential phase

In this study the growth rate of *P. tricornutum* was lower than that of *C. neogracile* during exponential phase. *P. tricornutum* is larger than *C. neogracile* by up to ~3 times. Banse (1982) and Sarthou et al. (2005) observed that larger diatoms grow slower than smaller ones because the uptake and assimilation of nutrients is faster for the smaller cells.

The average specific growth rate of *P. tricornutum* was approximately the same between exponential phase 1 and 2, but that of *C. neogracile* was different. This difference in growth rate observed for *C. neogracile* may be caused by its growth cycle. Microalgae can indeed undergo both sexual and asexual reproduction. Asexual reproduction (vegetative) involves the progression of cell division. During vegetative process, the average size of the diatom frustule decreases (Chisholm and Costello, 1980; Round et al., 1990). The frustule is made up of two, slightly unequal siliceous thecae fitting to each other as a lid and a box. During cell division, each daughter cell inherits one maternal theca (which forms the lid), and synthesizes its smaller hypotheca (which forms the box) (Round et al., 1990). This process of synthesising smaller hypotheca from one generation to another reduces the cell size of the diatom. To restore its cell size, the diatom onsets sexual reproduction (Chepurnov et al., 2005). Sexual reproduction involves the formation of auxospore. Auxospores are the cells that possess a wall structure which lacks the siliceous frustule. The absence of a siliceous wall enables the cell to expand to its specific initial size. The growth rate increases when the cells are transformed from pre to post–auxospore and the minimum growth rate is

attained when the cells are bigger (vegetative cell division) (Chepurnov et al., 2005; D'Alelio et al., 2009). Within the same species of diatom, the maximum growth rate can differ by a factor of 2 due to different growth cycles (Chisholm and Costello, 1980). The cell volume of *C. neogracile* was indeed smaller during exponential phase 2 (66 ± 8 μm^3, n=18) when the growth rate was higher than during exponential phase 1 (97 ± 1 μm^3, n=10) when the growth rate was low (t-test, $p<0.05$). *C. neogracile* may thus have to undergo sexual reproduction during exponential phase 1.

4.1.2 During CO_2 and nitrate limitation

The growth rate of *Phaeodactylum tricornutum* and *Chaetoceros neogracile* decreased when the cultures were limited with respect to CO_2 and nitrate. Other studies also revealed that the growth rate of diatoms may depend on the internal concentration of the limiting nutrient. Examples are: phosphorus for *Phaeodactylum tricornutum* (Kuenzler and Ketchum, 1962), CO_2 for *Thalassiosira pseudonana* and *Thalassiosira oceanica* (Chen and Durbin, 1994), silicate, phosphate, nitrate and CO_2 for *Thalassiosira pseudonana* (Bucciarelli and Sunda, 2003).

During CO_2 limitation the change of pH was similar for both species, i.e. 0.28 for *P. tricornutum* and 0.27 for *C. neogracile.* However, the change of biomass was higher for *P. tricornutum* (1.6×10^5 cells mL^{-1}) than for *C. neogracile* (8.5×10^4 cells mL^{-1}). This suggests a lower carbon requirement per cell and per cell volume for *P. tricornutum* than for *C. neogracile*. According to the findings of Goldman et al. (1982) on different cultures of marine microalgae, *P. tricornutum* has the ability to sustain its growth at a higher pH (~10.3), i.e. at very low concentration of CO_2 as compared to other species. This enables *P. tricornutum* to dominate other species in the marine environment (Goldman et al., 1982).

It was also found that for cultures during CO_2 limitation, there was a delay in changing growth rate after limitation. The cultures were limited by CO_2 from day 5 (after NaOH addition), but the growth rate was still maximum on day 6 and dramatically decreased only on day 7 (Figure 3.5a and b). This may be caused by the cells still having enough carbon to support growth for a few hours before

becoming limited. A study done by Kuenzler and Ketchum (1962) on *P. tricornutum* found that this diatom can accumulate phosphorus and use this storage to continue to divide for hours with no phosphorus in its medium (i.e. less than 24 hours). This could be the case for carbon in this study.

4.2 Bromoform production during different stages of growth rate

Both *C. neogracile* and *P. tricornutum* produced bromoform during their exponential phase. This was also found by Colomb et al. (2008), however Colomb et al. (2008) observed 16 times more bromoform production by *C. neogracile* than by *P. tricornutum*, while this study observed only ~3 times more bromoform produced by *C. neogracile* than by *P. tricornutum*. The higher rates observed by Colomb et al. (2008) might be caused either by direct bacterial production; since their cultures were not axenic or due to bacterially-induced algae defence (McConnell and Fenical, 1977; Manley, 2002). Since bacteria are also known to produce organobromine compounds (Goodwin et al., 1997b; Gribble, 2003) this could explain some of the variability seen. The presence of bacteria in the culture might stimulate the algae to produce more bromoform to serve as a chemical defence against them. During this study, the culture was kept axenic and provides strong evidence that diatoms can produce bromoform under axenic conditions.During this study, the culture was kept axenic and provides strong evidence that diatoms can produce bromoform under axenic conditions. This means that the link between oxidative stress in phytoplankton and bromoform production, as hypothesized by Pedersén et al. (1996) for macroalgae, can be investigated.

4.2.1 Cells metabolic imbalances and increase in oxidative stress

Nutrient limitation causes metabolic imbalances. During CO_2 limitation there is an increase in the demand of energy (ATP) as a result of extra requirement for active transport of inorganic carbon. Some of the impaired metabolic activities associated with nitrate limitation are: impaired light harvesting and electron transport within the photosynthetic apparatus, CO_2 fixation within the Calvin Benson cycle and enzymatic elimination of reactive oxygen species (Bucciarelli and Sunda, 2003).

Metabolic imbalances further lead to oxidative stress and decreased growth rate (Bucciarelli and Sunda, 2003). Oxidative stress is caused by the production and accumulation of ROS beyond the capacity of an organism to reduce them, which can ultimately result in cell death (Vardi et al., 1999; Sunda et al., 2002; Lesser, 2006). Reactive oxygen species (ROS) is a collective term that includes both oxygen radicals, *e.g.* superoxide ($O_2^{\bullet\bullet}$), hydroxyl ($OH^{\bullet}$), peroxyl ($RO_2^{\bullet}$), and hydroperoxyl ($HO_2^{\bullet}$) radicals, and certain non-radical oxidizing agents, *e.g.* hydrogen peroxide (H_2O_2) and hypochlorous acid (HOCl), that can easily be converted into radicals (Halliwell and Gutteridge, 1989; Lesser, 2006)). ROS are produced during the metabolism of normal cells and are involved in processes like enzymatic reactions, mitochondrial electron transport, and signal transduction (Lesser, 2006). Accumulation of ROS, for example due to nutrient limitation and metabolic imbalances, can have lethal effects on the cell, i.e. shrinking of the protoplast and fragmentations of deoxyribonucleic acid (DNA) (Vardi et al., 1999).

The presence of reducing conditions inside the cells helps to prevent free radical-mediated damage. These reducing conditions are maintained by the action of antioxidant enzymes like superoxide dismutase (SOD) and catalase (Bayr, 2005). For example, SOD converts $O_2^{\bullet\bullet}$ into H_2O_2 which can further be converted to water molecules by the action of catalases. Under oxidative stress, primary producers increase the production of antioxidants and antioxidant enzymes (Lesser and Shick, 1989; Sunda et al., 2007; Harada et al., 2009).

Bromoperoxidase is among the antioxidant enzymes that have been found in diatoms (Moore et al., 1996). This antioxidant enzyme produces bromoform when reacted with H_2O_2 (Pedersén et al., 1996; Manley and Barbero, 2001). Bromoform should thus increase under increased oxidative stress which occurs during nutrient limitation.

4.2.2 The link between oxidative stress and bromoform production

Although production of bromoform was observed during CO_2 limitation, it significantly decreased when compared with the exponential phase for both species (t-test, $p<0.05$ for *P .tricornutum* and $p=0.05$ for *C. neogracile*). A decrease

in bromoform per cell from the exponential phase to the senescent phase was also observed by Moore et al. (1996), although the senescent phase could not be attributed to a specific nutrient. During NO_3 limitation, the bromoform concentration in the cultures never exceeded the control values. This suggests that *P. tricornutum* did not produce bromoform under nitrate limitation.

Pedersén et al. (1996) hypothesized that bromoform is a by-product of the action of the antioxidant enzyme bromoperoxidase under oxidative stress. Based on the study done on seaweed by this researcher, it was found that, in some macroalgae brominating reactions by peroxidases scavenge H_2O_2, which lowers oxidative stress. Vardi et al. (1999) and Sunda et al. (2002) measured an increase of ROS with decreasing CO_2 availability for the species *Peridium gatunense* and *Thalassiosira pseudonana* respectively. The study of Vardi et al. (1999) was conducted with a natural lake phytoplankton bloom, where the measurements of pH (as a proxy for CO_2) and H_2O_2 were monitored. Sunda et al. (2002) conducted CO_2 limited culture studies of *Thalassiosira pseudonana*. They observed that antioxidants increased during CO_2 limitation, similar to that observed when H_2O_2 was added directly to the cultures.

Nitrate limitation also results in metabolic imbalances (Bucciarelli and Sunda, 2003), and an increase in the concentration of ROS (Falkowski et al., 1998; Harada et al,. 2009). CO_2 and nitrate limitation in this study's cultures decreased the growth rate and this may be associated with the increase in ROS (Bucciarelli and Sunda, 2003). Since the production of bromoform is related to the increase of ROS, then the decrease in growth rate should be inversely related to the bromoform production. However, our study shows that the decrease in bromoform production was related with the decrease in growth rate under CO_2 limitation, with no production during nitrate limitation.

The reason for the decrease in bromoform production with the increase in ROS may be attributed to the absence or low production of the enzyme bromoperoxidase. This enzyme is made up of protein, *i.e.* it is rich in nitrogen (Littlechild et al., 2009; Johnson et al., 2011), so any interference on nitrate uptake (during CO_2 limitation: Bucciarelli and Sunda, 2003), or the absence of

nitrate (during nitrate limitation), may cause a decrease of its production or of its activity.

Under nitrate limitation, all processes dependent on nitrate rich proteins slow down (*i.e.* light harvesting and electron transport within the photosynthetic apparatus, CO_2 fixation within the Calvin Benson cycle and enzymatic elimination of reactive oxygen species) (Bucciarelli and Sunda, 2003). A decrease in the concentration of the nitrate rich enzyme ribulose bisphosphate carboxylase (Rubisco) was observed by Berges and Falkowski (1998) during nitrate limitation of the diatom *Thalassiosira weissflogii*.

During CO_2 limitation, there is also more requirement of the enzyme carbonic anhydrase. This is caused by the increase in demand of energy (ATP) as a result of extra requirement for active transport of inorganic carbon. The transport requires the conversion of HCO_3 to CO_2 at the cell surface which takes place under the presence of carbonic anhydrase enzyme. The enzyme requires nitrate to be produced. The requirement of this enzyme at higher rates may limit the production of other nitrate rich enzymes, including bromoperoxidase, *i.e*. the rate of bromoform production.

Both CO_2 and nitrate limitation may thus decrease the production and/or activity of bromoperoxidase and production of bromoform, with a more severe effect of nitrate limitation than of CO_2 limitation.

CHAPTER 5

CONCLUSION AND PERSPECTIVES

According to our study, bromoperoxidase concentration/activity may require nitrogen, and any limitation decreasing nitrogen uptake may decrease bromoform production. The decreased concentration/activity of bromoperoxidase may be compensated by other antioxidants that do not require nitrogen (*e.g.* the sulphur containing antioxidant dimethylsulfoniopropionate (DMSP) (Bucciarelli and Sunda, 2003). In this study we did not measure DMSP or bromoperoxidase concentration/activity. This presents future research questions: 1) Does bromoperoxidase concentration or activity decrease with nutrient limitation linked to nitrogen limitation (i.e. CO_2 or nitrate limitation)? 2) Is there any increase in concentration of other antioxidants to compensate for decreased bromoperoxidase concentration/activity?

There is also a need to broaden the study of bromoform production under specific nutrient variations, and with different species of phytoplankton in order that we may better understand the conditions that regulate bromoform production. Ultimately, such information can be incorporated in models that can make predictions of bromoform concentration and its impact on the destruction of ozone.

REFERENCES

ANBAR, A., YUNG, Y. and CHAVEZ, F., 1996. Methyl bromide: Ocean sources, ocean sinks, and climate sensitivity. *Global Biogeochemical Cycles,* **10**(1), pp. 175-190.

ATLAS, E., POLLOCK, W., GREENBERG, J., HEIDT, L. and THOMPSON, A., 1993. Alkyl nitrates, nonmethane hydrocarbons, and halocarbon gases over the equatorial Pacific Ocean during SAGA 3. *Journal of geophysical research,* **98**(D9), pp. 16933-16947.

BANSE, K., 1982. Cell volumes, maximal growth rates of unicellular algae and ciliates, and the role of ciliates in the marine pelagial. *Limnology and Oceanography,* **27**(6), pp. 1059-1071.

BARTUAL, A., GALVEZ, J.A. and OJEDA, F., 2008. Phenotypic response of the diatom *Phaeodactylum tricornutum* Bohlin to experimental changes in the inorganic carbon system. *Botanica Marina,* **51**(5), pp. 350-359.

BAYR, H., 2005. Reactive oxygen species. *Critical Care Medicine,* **33**(12), pp. S498

BERGES, J.A. and FALKOWSKI, P.G., 1998. Physiological stress and cell death in marine phytoplankton: Induction of proteases in response to nitrogen or light limitation. *Limnology and Oceanography*, **43**(1), pp. 129-135.

BENDSCHNEIDER, K. and ROBINSON, R.J., 1952. A new spectrophotometric method for the determination of nitrite in sea water. *Journal of Marine Research*, **11**, pp. 87-96.

BOTTENHEIM, J.W., BARRIE, L.A., ATLAS, E., HEIDT, L.E., NIKI, H., RASMUSSEN, R.A. and SHEPSON, P.B., 1990. Depletion of lower tropospheric ozone during Arctic spring: The Polar Sunrise Experiment 1988. *J.geophys.Res,* **95**(18), pp. 518-555.

BRIDGEMAN, C., PYLE, J. and SHALLCROSS, D., 2000. A three-dimensional model calculation of the ozone depletion potential of 1-bromopropane (1-C_3H_7Br). *Journal of geophysical research,* **105**(D21), pp. 26493-26502.

BUCCIARELLI, E. and SUNDA, W.G., 2003. Influence of CO_2, nitrate, phosphate, and silicate limitation on intracellular dimethylsulfoniopropionate in batch cultures of the coastal diatom *Thalassiosira pseudonana*. *Limnology and Oceanography,* **48**(6), pp. 2256-2265.

BUCCIARELLI, E., SUNDA, W.G., BELVISO, S. and SARTHOU, G., 2007. Effect of the diel cycle on production of dimethylsulfoniopropionate in batch cultures of *Emiliania huxleyi*. *Aquatic Microbial Ecology,* **48**(1), pp. 73-81

BUTLER, J.H., KING, D.B., LOBERT, J.M., MONTZKA, S.A., YVON-LEWIS, S.A., HALL, B.D., WARWICK, N.J., MONDEEL, D.J., AYDIN, M. and ELKINS, J.W., 2007. Oceanic distributions and emissions of short-lived halocarbons. *Global Biogeochem.Cycles,* **21**(1), pp. GB1023

CARPENTER, L. and LISS, P., 2000. On temperate sources of bromoform and other reactive organic bromine gases. *Journal of geophysical research,* **105**(D16), pp. 20539-20547.

CHAPMAN, S., 1930. A theory of upper-atmospheric ozone. *Memoirs of the Royal Meteorological Society*, **3,** pp. 103-125.

CHEN, C. and DURBIN, E.G., 1994. Effects of pH on the growth and carbon uptake of marine phytoplankton. *Marine Ecology-Progress Series,* **109**(1), pp. 83-94.

CHEPURNOV, V.A., MANN, D.G., SABBE, K., VANNERUM, K., CASTELEYN, G., VERLEYEN, E., PEPERZAK, L. and VYVERMAN, W., 2005. Sexual reproduction, mating system, chloroplast dynamics and abrupt cell size reduction in *Pseudonitzschia pungens* from the North Sea (Bacillariophyta). *European Journal of Phycology,* **40**(4), pp. 379-395.

CHISHOLM, S.W. and COSTELLO, J.C., 1980. Influence of environmental factors and population composition on the timing of cell division in *Thalassiosira fluviatilis* (Bacillariophyceae) grown on light/dark cycles. *Journal of Phycology,* **16**(3), pp. 375-383.

CHUCK, A.L., TURNER, S.M. and LISS, P.S., 2005. Oceanic distributions and air-sea fluxes of biogenic halocarbons in the open ocean. *Journal of geophysical research,* **110**(C10), pp. C10022.

COLLÉN, J., EKDAHL, A., ABRAHAMSSON, K. and PEDERSÉN, M., 1994. The involvement of hydrogen peroxide in the production of volatile halogenated compounds by *Meristiella gelidium*. *Phytochemistry,* **36**(5), pp. 1197-1202.

COLOMB, A., YASSAA, N., WILLIAMS, J., PEEKEN, I. and LOCHTE, K., 2008. Screening volatile organic compounds (VOCs) emissions from five marine phytoplankton species by head space gas chromatography/mass spectrometry (HS-GC/MS). *J.Environ.Monit,* **10**(3), pp. 325-330.

CUESTA, J. L and MANLEY, S.L., 2009. Iodine assimilation by marine diatoms and other phytoplankton in nitrate-replete conditions. *Limnol.Oceanogr,* **54**(5), pp. 1653-1664.

D'ALELIO, D., AMATO, A., LUEDEKING, A. and MONTRESOR, M., 2009. Sexual and vegetative phases in the planktonic diatom *Pseudonitzschia multistriata*. *Harmful Algae,* **8**(2), pp. 225-232.

DIENÉRT, F. and WANDENBULCKE, F., 1923. On the determination of silica in water. *Compt.Rend,* **176**, pp. 1478-1480.

DVORTSOV, V.L., GELLER, M.A., SOLOMON, S., SCHAUFFLER, S.M., ATLAS, E.L. and BLAKE, D.R., 1999. Rethinking reactive halogen budgets in the midlatitude lower stratosphere. *Geophysical Research Letters,* **26**(12), pp. 1699-1702.

EPPLEY, R.W., 1972. Temperature and phytoplankton growth in the sea. *Fish.Bull,* **70**(4), pp. 1063-1085.

FAHEY, D. and RAVISHANKARA, A., 1999. Summer in the stratosphere. *Science,* **285**(5425), pp. 208.

FALKOWSKI, P.G., BARBER, R.T. and SMETACEK, V., 1998. Biogeochemical controls and feedbacks on ocean primary production. *Science,* **281**(5374), pp. 200-206.

FOGELQVIST, E. and KRYSELL, M., 1991. Naturally and anthropogenically produced bromoform in the Kattegatt, a semi-enclosed oceanic basin. *Journal of Atmospheric Chemistry,* **13**(4), pp. 315-324.

GOLDMAN, J.C., AZOV, Y., RILEY, C.B. and DENNETT, M.R., 1982. The effect of pH in intensive microalgal cultures. I. Biomass regulation. *Journal of experimental marine biology and ecology,* **57**(1), pp. 1-13.

GOODWIN, K.D., NORTH, W.J. and LIDSTROM, M.E., 1997a. Production of bromoform and dibromomethane by giant kelp: Factors affecting release and comparison to anthropogenic bromine sources. *Limnology and Oceanography,* **42**(8), pp. 1725-1734.

GOODWIN, K.D., LIDSTROM, M.E. and OREMLAND, R.S., 1997b. Marine bacterial degradation of brominated methanes. *Environmental science & technology,* **31**(11), pp. 3188-3192.

GREENFIELD, L. J. AND KALBER, F. A., 1954. Inorganic phosphate measurements in sea water. *Bull. Mar. Sci. Gulf and Caribbean*, **4**, pp. 323-135.

GRIBBLE, G.W., 2003. The diversity of naturally produced organohalogens. *Chemosphere,* **52**(2), pp. 289-297.

GRIBBLE, G.W., 1999. The diversity of naturally occurring organobromine compounds. *Chem.Soc.Rev.,* **28**(5), pp. 335-346.

GSCHWEND, P.M., MACFARLANE, J.K. and NEWMAN, K.A., 1985. Volatile halogenated organic compounds released to seawater from temperate marine macroalgae. *Science,* **227**(4690), pp. 1033-1035.

GUICHERIT, R. and ROEMER, M., 2000. Tropospheric ozone trends. *Chemosphere Global Change Science,* **2**(2), pp. 167-183.

GUILLARD, R.R.L., 1975. Culture of phytoplankton for feeding marine invertebrates. p. 29-60. *In* W. L. Smith and M. H. Chanley [eds.], Culture of marine invertebrate animals. Plenum Pub., New York.

HALLIWELL, B. and GUTTERIDGE, J., 1989. Free radicals, ageing and disease. Clarendon Press, Oxford, pp. 416–508.

HARADA, H., VILA-COSTA, M., CEBRIAN, J. and KIENE, R.P., 2009. Effects of UV radiation and nitrate limitation on the production of biogenic sulfur compounds by marine phytoplankton. *Aquatic Botany,* **90**(1), pp. 37-42.

HENSE, I. and QUACK, B., 2009. Modeling the vertical distribution of bromoform in the upper water column of the tropical Atlantic Ocean. *Biogeosciences (BG),* **6**(4), pp. 535-544.

HONAGANAHALLI, P.S. and SEIBER, J.N., 1997. Health and environmental concerns over the use of fumigants in agriculture: The case of methyl bromide. *ACS Symposium Series 1997, ACS Publications,* **652**, pp. 1-13.

JOHNSON, T.L., PALENIK, B. and BRAHAMSHA, B., 2011. Characterization of a functional vanadium dependent bromoperoxidase in the marine *Cyanobacterium synechococcus* sp. CC93111. *Journal of Phycology,* **47**(4), pp. 792-801

KELLER, M.D., BELLOWS, W.K. and GUILLARD, R.R.L., 1988. Microwave treatment for sterilization of phytoplankton culture media. *Journal of experimental marine biology and ecology,* **117**(3), pp. 279-283.

KRUPA, S.V. and MANNING, W.J., 1988. Atmospheric ozone: Formation and effects on vegetation. *Environmental Pollution,* **50**(1-2), pp. 101-137.

KRYSELL, M., 1991. Bromoform in the Nansen Basin in the Arctic Ocean. *Marine Chemistry,* **33**(1-2), pp. 187-197.

KUENZLER, E.J. and KETCHUM, B.H., 1962. Rate of phosphorus uptake by *Phaeodactylum tricornutum*. *The Biological bulletin,* **123**(1), pp. 134-145.

LACIS, A.A., WUEBBLES, D.J. and LOGAN, J.A., 1990. Radiative forcing of climate by changes in the vertical distribution of ozone. *Journal of Geophysical Research,* **95**(D7), pp. 9971-9981.

LATURNUS, F., WIENCKE, C. and KLÖSER, H., 1996. Antarctic macroalgae: Sources of volatile halogenated organic compounds. *Marine environmental research,* **41**(2), pp. 169-181.

LESSER, M.P., 2006. Oxidative stress in marine environments: Biochemistry and physiological ecology. *Annual Review of Physiology,* **68**, pp. 253-278.

LESSER, M. and SHICK, J., 1989. Effects of irradiance and ultraviolet radiation on photoadaptation in the zooxanthellae of *Aiptasia pallida*: Primary production, photoinhibition, and enzymic defenses against oxygen toxicity. *Marine Biology,* **102**(2), pp. 243-255.

LITTLECHILD, J., GARCIA RODRIGUEZ, E. and ISUPOV, M., 2009. Vanadium containing bromoperoxidase: Insights into the enzymatic mechanism using X-ray crystallography. *Journal of inorganic biochemistry,* **103**(4), pp. 617-621.

LIU, H., JACOB, D.J., CHAN, L.Y., OLTMANS, S.J., BEY, I., YANTOSCA, R.M., HARRIS, J.M., DUNCAN, B.N. and MARTIN, R.V., 2002. Sources of tropospheric ozone along the Asian Pacific Rim: An analysis of ozonesonde observations. *J.geophys.Res,* **107**(21).

MANLEY, S.L., 2002. Phytogenesis of halomethanes: A product of selection or a metabolic accident? *Biogeochemistry,* **60**(2), pp. 163-180.

MANLEY, S.L. and BARBERO, P.E., 2001. Physiological constraints on bromoform ($CHBr_3$) production by *Ulva lactuca* (Chlorophyta). *Limnology and Oceanography,* **46**(6), pp. 1392-1399.

MANLEY, S.L., GOODWIN, K. and NORTH, W.J., 1992. Laboratory production of bromoform, methylene bromide, and methyl iodide by macroalgae and distribution in near shore southern California waters. *Limnology and Oceanography,* **37**(8), pp. 1652-1659.

MARTINO, A.D., MEICHENIN, A., SHI, J., PAN, K. and BOWLER, C., 2007. Genetic and phenotypic characterization of *Phaeodactylum tricornutum* (Bacillariophyceae) accessions. *Journal of Phycology,* **43**(5), pp. 992-1009.

MCCONNELL, O. and FENICAL, W., 1977. Halogen chemistry of the red alga *Asparagopsis*. *Phytochemistry,* **16**(3), pp. 367-374.

MCGIVERN, W.S., JOSEPH, S. and SIMON, W., 2002. Investigation of the atmospheric oxidation pathways of bromoform: Initiation via OH/Cl reactions. *The Journal of Physical Chemistry,* **106**(26), pp. 6395-6400.

MOORE, R., TOKARCZYK, R. and GEEN, C., 1993. Sources of organobromines to the Arctic atmosphere. *The Tropospheric Chemistry of Ozone in the Polar Regions,* NATO ASI Set. Subset. I, Springer-Verlag, New York, vol. 7, pp. 235-250.

MOORE, R., WEBB, M., TOKARCZYK, R. and WEVER, R., 1996. Bromoperoxidase and iodoperoxidase enzymes and production of halogenated methanes in marine diatom cultures. *Journal of geophysical research,* **101**(C9), pp. 20899-20908.

MURPHY, J. and RILEY, J., 1958. A single-solution method for the determination of soluble phosphate in sea water. *Journal of the Marine Biological Association of the United Kingdom,* **37**(01), pp. 9-14.

NELSON, D.M., TRÉGUER, P., BRZEZINSKI, M.A., LEYNAERT, A. and QUÉGUINER, B., 1995. Production and dissolution of biogenic silica in the ocean: Revised global estimates, comparison with regional data and relationship to biogenic sedimentation. *Global Biogeochemical Cycles,* **9** (3), pp. 359.

NIELSEN, J.E. and DOUGLASS, A.R., 2001. A simulation of bromoform's contribution to stratospheric bromine. *Journal of geophysical research,* **106**(D8), pp. 8089-8100.

NOCTOR, G. and FOYER, C.H., 1998. Ascorbate and glutathione: Keeping active oxygen under control. *Annual review of plant biology,* **49**(1), pp. 249-279.

OLTMANS, S., SCHNELL, R., SHERIDAN, P., PETERSON, R., LI, S.M., WINCHESTER, J., TANS, P., STURGES, W., KAHL, J. and BARRIE, L., 1989. Seasonal surface ozone and filterable bromine relationship in the high Arctic. *Atmospheric Environment (1967),* **23**(11), pp. 2431-2441.

PALMER, C.J. and REASON, C.J., 2009. Relationships of surface bromoform concentrations with mixed layer depth and salinity in the tropical oceans. *Global Biogeochemical Cycles,* **23**(2), pp. GB2014.

PAUL, C. and POHNERT, G., 2011. Production and role of volatile halogenated compounds from marine algae. *Natural product reports,* **28**(2), pp. 186-195.

PEDERSÉN, M., COLLÉN, J., ABRAHAMSSON, K. and EKDAHL, A., 1996. Production of halocarbons from seaweeds: An oxidative stress reaction. *Scientia Marina,* **60**, pp. 257–263.

PIDWIRNY, M., 2006. The ozone layer. *Fundamentals of physical geography, 2nd edition*. Date Viewed. *(http://www.physicalgeography.net/fundamentals/7e.html)*

PRUDER, G.D. and BOLTON, E.T., 1979. The role of CO_2 enrichment of aerating gas in the growth of an estuarine diatom. *Aquaculture,* **17**(1), pp. 1-15.

QUACK, B. and WALLACE, D., 2003. Air-sea flux of bromoform: Controls, rates, and implications. *Global Biogeochem.Cycles,* **17**(1), pp. 1023.

ROUND, F.E., CRAWFORD, R.M. and MANN, D.G., 1990. The diatoms: Biology & morphology of the genera. Cambridge Univ Pr.

SALAWITCH, R.J., 2006. Biogenic bromine. *Nature,* **439**(7074), pp. 275-277.

SARTHOU, G., TIMMERMANS, K.R., BLAIN, S. and TRÉGUER, P., 2005. Growth physiology and fate of diatoms in the ocean: A review. *Journal of Sea Research,* **53**(1), pp. 25-42.

SCARRATT, M. and MOORE, R., 1998. Production of methyl bromide and methyl chloride in laboratory cultures of marine phytoplankton II. *Marine Chemistry,* **59**(3-4), pp. 311-320.

SCARRATT, M. and MOORE, R., 1996. Production of methyl chloride and methyl bromide in laboratory cultures of marine phytoplankton. *Marine Chemistry,* **54**(3-4), pp. 263-272.

SCHAUFFLER, S., ATLAS, E., BLAKE, D., FLOCKE, F., LUEB, R., LEE-TAYLOR, J., STROUD, V. and TRAVNICEK, W., 1999. Distributions of brominated organic compounds in the troposphere and lower stratosphere. *Journal of geophysical research,* **104**(D17), pp. 21513-21,535.

STURGES, W.T., ORAM, D.E., CARPENTER, L.J., PENKETT, S.A., ENGEL, A., 2000. Bromoform as a source of stratospheric bromine. *Geophysical Research Letters,* **27**(14), pp. 2081-2084.

STRICKLAND, J.D.H., PARSONS, T.R., 1965. A manual of sea water analysis. *2nd ed. Revised. Fisheries Research Board of Canada*, **125**, pp. 203

SUNDA, W.G., HARDISON, R., KIENE, R.P., BUCCIARELLI, E. and HARADA, H., 2007. The effect of nitrogen limitation on cellular DMSP and DMS release in marine phytoplankton: Climate feedback implications. *Aquatic Sciences-Research Across Boundaries,* **69**(3), pp. 341-351.

SUNDA, W., KIEBER, D., KIENE, R. and HUNTSMAN, S., 2002. An antioxidant function for DMSP and DMS in marine algae. *Nature,* **418**(6895), pp. 317-320.

SUNDA, W.G. and HUNTSMAN, S.A., 1995. Iron uptake and growth limitation in oceanic and coastal phytoplankton. *Marine Chemistry,* **50**(1), pp. 189-206.

TOKARCZYK, R. and MOORE, R.M., 1994. Production of volatile organohalogens by phytoplankton cultures. *Geophysical Research Letters,* **21**(4), pp. 285-288.

VARDI, A., BERMAN-FRANK, I., ROZENBERG, T., HADAS, O., KAPLAN, A. and LEVINE, A., 1999. Programmed cell death of the dinoflagellate *Peridinium gatunense* is mediated by CO_2 limitation and oxidative stress. *Current Biology,* **9**(18), pp. 1061-1064.

WANG, W.C., LIANG, X.Z., DUDEK, M., POLLARD, D. and THOMPSON, S., 1995. Atmospheric ozone as a climate gas. *Atmospheric Research,* **37**(1-3), pp. 247-256.

WANG, W.C., PINTO, J.P., YUNG, Y.L. and NATIONAL AERONAUTICS AND SPACE ADMINISTRATION. GODDARD INST. FOR SPACE STUDIES, NEW YORK, NY, 1980. Climatic effects due to halogenated compounds in the Earth's atmosphere. *Journal of the Atmospheric Sciences,* **37**(2), pp. 333-338.

WARWICK, N., PYLE, J., CARVER, G., YANG, X., SAVAGE, N., O'CONNOR, F. and COX, R., 2006. Global modeling of biogenic bromocarbons. *Journal of geophysical research,* **111**(D24), pp. D24305.

WEVER, R., TROMP, M.G.M., KRENN, B.E., MARJANI, A. and VAN TOL, M., 1991. Brominating activity of the seaweed *Ascophyllum nodosum*: Impact on the biosphere. *Environmental science & technology,* **25**(3), pp. 446-449.

WOFSY, S.C., MCELROY, M.B. and YUNG, Y.L., 1975. The chemistry of atmospheric bromine. *Geophysical Research Letters,* **2**(6), pp. 215-218.

WORLD METEOROLOGICAL ORGANIZATION, 1999. Scientific Assessment of Ozone Depletion: 1998, Global Ozone Research and Monitoring Project Report No. 44, WMO, Geneva.

WUOSMAA, A.M. and HAGER, L.P., 1990. Methyl chloride transferase: A carbocation route for biosynthesis of halometabolites. *Science,* **249**(4965), pp. 160-162.

XU, D., FRANCISCO, J.S., HUANG, J. and JACKSON, W.M., 2002. Ultraviolet photodissociation of bromoform at 234 and 267nm by means of ion velocity imaging. *The Journal of chemical physics,* **117**(6), pp. 2578.

YANG, X., COX, R.A., WARWICK, N.J., PYLE, J.A., CARVER, G.D., O'CONNOR, F.M. and SAVAGE, N.H., 2005. Tropospheric bromine chemistry and its impacts on ozone: A model study. *Journal of geophysical research,* **110**(D23), pp. D23311.

YOKOUCHI, Y., HASEBE, F., FUJIWARA, M., TAKASHIMA, H., SHIOTANI, M., NISHI, N., KANAYA, Y., HASHIMOTO, S., FRASER, P. and TOOM-SAUNTRY, D., 2005. Correlations and emission ratios among bromoform, dibromochloromethane, and dibromomethane in the atmosphere. *Journal of geophysical research,* **110**(D23), pp. D23309.

YUNG, Y., PINTO, J., WATSON, R. and SANDER, S., 1980. Atmospheric bromine and ozone perturbations in the lower stratosphere. *Journal of the Atmospheric Sciences,* **37**(2), pp. 339-353.

ANNEX

Table 1(a): *P. tricornutum* growth rate and macronutrients concentrations during preliminary experiment

Time(d)	μ(d^{-})	pH	NO_3^- (μM)	PO_4-P (μM)	SiO_4-Si (μM)
0.00	----	----	----	----	----
1.01	1.73	7.82	92.20	28.54	126.63
2.08	0.95	8.00	91.82	28.54	126.44
2.96	1.70	8.00	90.08	28.54	124.98
3.97	0.71	8.10	87.06	28.54	124.47
5.00	0.77	8.17	78.44	23.30	122.41
6.00	0.93	8.28	50.50	21.11	112.39
7.00	1.31	8.64	1.45	14.29	101.65

Table 1(b): *C. neogracile* growth rate and macronutrients concentrations during preliminary experiment

Time(d)	μ(d^{-})	pH	NO_3^- (μM)	PO_4-P (μM)	SiO_4-Si (μM)
0.00	----	----	----	----	----
1.01	2.37	7.98	91.48	28.54	121.05
2.08	0.94	8.03	90.97	28.54	120.45
2.96	1.32	8.11	84.70	23.46	118.69
3.97	0.97	8.25	67.82	21.65	102.37
5.00	2.12	8.68	1.56	14.97	24.85

Table 2(a): P. *tricornutum* growth rate and macronutrients concentrations during exponential phase (1)

Culture sample	Time(d)	μ(d^{-})	pH	NO_3^- (μM)	PO_4-P (μM)	SiO_4-Si (μM)
Sample 'A'	0.00	----	----	----	----	-----
	1.04	1.21	7.87	717.11	26.12	122.50
	2.05	1.35	7.86	715.81	26.64	121.26
	3.07	1.40	7.99	699.99	27.17	128.08
	4.00	1.27	8.12	646.21	25.33	132.42
	5.01	1.26	8.29	647.99	24.28	130.35
	6.05	1.16	9.22	702.29	30.58	131.80
Sample 'B'	0.00	----	----	----	----	-----
	1.06	1.20	8.00	743.36	26.90	125.39
	2.06	1.34	8.00	684.68	26.64	125.19
	3.09	1.36	8.02	671.80	27.43	131.18
	4.03	1.21	8.13	717.61	28.22	130.35
	5.03	1.33	8.29	596.00	24.28	131.80
	6.06	1.22	9.17	606.59	30.31	131.59
Sample 'C'	0.00	----	----	----	----	-----
	1.07	1.23	7.87	696.74	26.38	110.31
	2.07	1.37	7.86	739.78	26.64	110.72
	3.10	1.34	7.99	721.03	27.95	127.46
	4.05	1.24	8.12	691.20	25.33	128.70
	5.05	1.40	8.29	702.93	23.23	130.35
	6.08	1.08	9.22	760.48	30.84	130.14

Table 2(b): *C. neogracile* growth rate and macronutrients concentrations during exponential phase (1)

Culture sample	Time(d)	μ(d^{-})	pH	NO_3^- (μM)	PO_4-P (μM)	SiO_4-Si (μM)
Sample 'A'	0.00	----	----	----	----	-------
	1.00	1.52	7.91	790.14	28.22	103.70
	2.01	1.44	7.86	751.19	27.69	106.80
	3.03	1.43	7.89	761.45	27.69	105.76
	4.06	1.41	8.06	714.50	26.38	86.96
	5.08	1.81	8.49	724.13	21.81	79.02
	5.99	1.40	9.60	874.27	20.87	127.87
Sample 'B'	0.00	-----	------	------	------	------
	1.01	1.33	7.88	841.00	29.27	110.52
	2.02	1.27	7.84	792.59	28.48	105.14
	3.05	1.17	7.87	801.72	29.27	102.25
	4.08	1.48	7.95	764.06	28.74	96.26
	5.09	1.38	8.21	800.74	27.17	89.86
	6.00	1.13	9.35	705.71	28.38	149.15
Sample 'C'	0.00	-----	-----	-------	-----	------
	1.03	1.30	7.95	813.95	27.95	129.32
	2.03	1.09	7.91	772.05	27.95	112.17
	3.06	1.13	7.93	783.95	29.00	108.04
	4.10	1.02	8.02	779.88	28.74	100.19
	5.11	1.40	8.23	737.01	24.54	74.57
	6.03	1.70	9.19	723.49	28.94	87.28

Table 3(a): *P. tricornutum* growth rate and macronutrients concentrations during exponential phase (2)

Culture sample	Time(d)	μ(d^{-})	pH	NO_3^- (μM)	PO_4-P (μM)	SiO_4-Si (μM)
Sample 'A'	0.00	------	------	------	------	------
	2.92	1.41	8.03	------	------	------
	3.78	1.32	8.10	------	-------	------
	4.77	1.20	8.13	734.43	26.38	134.90
	5.78	1.23	8.12	455.61	22.70	126.84
	6.77	1.41	8.25	265.07	46.33	182.21
	7.72	1.08	8.05	61.30	80.27	253.29
Sample 'B'	0.00	-----	------	------	------	------
	2.92	1.41	8.03	------	------	------
	3.78	1.32	8.10	------	------	------
	4.78	1.21	8.15	858.58	28.22	134.90
	5.80	1.21	8.33	426.65	23.75	126.84
	6.78	1.31	8.27	253.62	44.75	182.21
	7.74	1.15	8.13	52.17	74.15	253.29

Table 3(b): *C. neogracile* growth rate and macronutrients concentrations during exponential phase (2)

Culture sample	Time(d)	μ(d^{-})	pH	NO_3^- (μM)	PO_4-P (μM)	SiO_4-Si (μM)
Sample 'A'	0.00	------	------	------	------	------
	2.92	2.32	7.96	-----	------	-----
	3.78	2.08	8.27	------	------	-----
	4.79	1.75	8.15	715.64	28.74	160.31
	5.81	1.91	8.34	676.85	42.91	233.45
	6.80	1.93	8.18	2265.93	94.88	392.13
Sample 'B'	0.00	------	------	------	------	-----
	2.92	2.32	7.96	------	------	------
	3.78	2.08	8.27	------	------	------
	4.80	1.68	8.04	760.31	29.79	139.24
	5.82	2.08	8.30	603.18	52.36	217.13
	6.81	1.99	8.20	1817.01	96.46	376.01

Table 4(a): *P. tricornutum* macronutrients concentrations during CO_2 limitation phase

Culture sample	Time(d)	μ(d^-)	pH	NO_3^- (μM	PO_4-P (μM)	SiO_4-Si (μM)
Sample 'A'	6.05	1.16	9.22	702.29	30.58	131.80
	6.99	0.82	9.60	594.22	19.03	153.90
	8.01	0.93	9.77	561.14	11.68	139.44
	9.02	0.09	9.76	368.60	15.53	138.80
	10.02	0.57	10.02	------	-------	-------
Sample 'B'	6.06	1.22	9.17	606.59	30.31	131.59
	7.00	0.45	9.61	472.44	19.47	143.37
	8.02	1.32	10.02	483.53	4.54	113.21
	9.04	0.00	9.86	456.14	8.95	91.37
	10.03	0.86	10.08	-------	-------	-------
Sample 'C'	6.08	1.08	9.11	760.48	30.84	130.14
	7.02	0.88	9.52	651.10	20.78	180.56
	8.05	0.79	9.74	566.83	15.97	157.42
	9.06	0.18	9.76	366.33	17.39	118.97
	10.03	0.22	9.96	------	------	------

Table 4(b): *C. neogracile* macronutrients concentrations during CO_2 limitation

Culture sample	Time(d)	μ(d^-)	pH	NO_3^- (μM)	PO_4-P (μM)	SiO_4-Si (μM)
Sample 'A'	5.99	1.40	9.60	874.27	20.87	127.87
	7.04	0.75	9.83	797.49	14.11	93.60
	8.05	0.51	9.78	748.27	15.42	61.23
	9.07	0.32	9.73	524.29	13.78	58.64
	9.99	0.15	10.10	------	-------	-------
Sample 'B'	6.00	1.38	9.35	705.71	28.38	149.15
	7.06	1.13	9.77	704.57	17.06	160.70
	8.07	0.54	9.68	666.27	15.42	330.37
	9.09	0.22	9.64	481.92	13.78	222.00
	10.00	0.19	10.08	------	-------	-------
Sample 'C'	6.03	1.70	9.19	723.49	28.94	87.28
	7.08	1.13	9.60	579.73	16.01	174.34
	8.09	0.55	9.50	756.78	18.04	183.68
	9.10	0.40	9.56	540.46	14.44	126.96
	10.01	0.36	10.01	------	------	-------

Table 5: *P. tricornutum* macronutrients concentrations during NO_3 limitation

Culture sample	Time(d)	μ(d^-)	pH	NO_3^- (μM)	PO_4-P (μM)	SiO_4-Si (μM)
Sample 'A'	7.72	1.08	8.05	61.30	80.27	253.29
	8.76	0.37	8.16	0	100.83	272.91
	9.76	0.39	8.16	0	65.72	391.28
	10.81	0.27	8.15	0	120.95	329.73
	11.75	0.10	8.17	------	-------	-------
Sample 'B'	7.74	1.15	8.13	52.17	74.15	252.87
	8.77	0.38	8.26	0	95.58	272.91
	9.78	0.41	8.25	0	84.32	412.77
	10.78	0.18	8.21	0	121.39	360.52
	11.77	0.14	8.24	------	-------	-------